2011

3-D Model Characterization and Identification from Intrinsic Landmarks

John L. Camp
Wright State University

3-D MODEL CHARACTERIZATION AND IDENTIFICATION FROM INTRINSIC LANDMARKS

A dissertation submitted in partial fulfillment of the
requirements for the degree of
Doctor of Philosophy

By

JOHN L. CAMP
B.S., University of Florida, 1998
M.S., Air Force Institute of Technology, 2002

_____

2011
Wright State University

DISSERTATION DEFENSE

WRIGHT STATE UNIVERSITY
School of Graduate Studies

16 November 2011

We hereby recommend that the dissertation prepared by John L. Camp titled 3-D Model Characterization and Identification from Intrinsic Landmarks be accepted in partial fulfillment of the requirements for the degree of Doctor of Philosophy.

Dissertation Director Arthur Goshtasby, Ph.D.	Committee Member Lang Hong, Ph.D., Electrical Engineering
Committee Member Jack Jean, Ph.D.	External Committee Member Kathleen Robinette, Ph.D., AFRL, WPAFB
Committee Member Thomas Wischoll, Ph.D.	
Director, CS&E Ph.D. Program Arthur Goshtasby, Ph.D.	Dean, School of Graduate Studies Andrew Hsu, Ph.D.

Abstract

Camp, John L. Ph.D., Computer Science and Engineering Ph.D. Program, Wright State University, 2011. 3-D Model Characterization and Identification from Intrinsic Landmarks

A method to automatically characterize and identify 3-D range scans based on intrinsic landmarks is presented. Intrinsic landmarks represent locally unique, intrinsic properties of a scanned surface, regardless of scale or rotation. The number, location, and characteristics of landmarks are used to characterize the scanned models. This method contains a selection process to identify stable, intrinsic landmarks for range scans as well as the identification of those scans. The selection process requires no user interaction or surface assumptions. It uses the principal curvatures at the range points to select the landmarks. First, a large number of landmarks are generated by fitting a bi-cubic polynomial surface to points surrounding each range point and calculating the principal curvatures at the range point. Points of locally extremum principal curvature are then considered candidate landmarks. Using a random sample and consensus (RANSAC) algorithm, candidate landmarks that match with landmarks in other scans of the same subject are selected as final, stable landmarks.

Our main goal is to provide a means to characterize models in a range data base. With several scans of each subject available in the data base, a number of stable landmarks are determined for each subject. The locations and characteristics of the landmarks are used to describe a subject and distinguish it from other subjects. The

main contribution of this work is considered to be the selection of unique and stable landmarks in a range scan and generation of a descriptor for each landmark that characterizes the intrinsic properties of the surface in the neighborhood of the landmark. The effectiveness of the method is presented through the successful identification of processed subjects and characterization of new subjects.

Table of Contents

List of Figures

PREFACE

This document has been approved for public release by the United States Air Force November 30, 2011. Case Number: 88ABW-2011-6205.

ACKNOWLEDGEMENTS

I wish I could individually express the appreciation I feel for all the friends, family, co-workers, fellow students, and professional faculty that have contributed to the success of my studies. Such a list would be far too long to include here; but for all of you not mentioned specifically, please know that I sincerely thank each of you for all your efforts on my behalf.

My thanks also go to the members of my committee for reviewing my previous written works and providing valuable feedback that improved the presentation and contents of those works. Dr. Wischgoll, your graphics course was one of my first doctoral classes and provided the foundation for my research code. I still remember your understanding and patience as I worked to rekindle my coding abilities, thank you.

I would not be here without the support from my Air Force colleagues, Dr. Michael Young, Dr. Kathleen Robinette, and Dr. Vincent Schmidt. Dr. Young, you encouraged me to begin this task, were always there to make sure I was comfortable in my decision and fully backed by the Air Force Research Laboratory. Dr. Robinette, it is your research that I have worked to contribute to and your data that enabled my studies. Thank you both for always being there for me. Vince, you were there at the beginning and the end; thank you for making sure I was in for the right reasons.

I would like to express my profound gratitude to my advisor, Dr. Ardy Goshtasby, for your support, patience, and encouragement throughout my graduate studies. Your technical and editorial advice was essential to the completion of this dissertation and has taught me innumerable lessons and insights on the workings of academic research in general.

It is with eternal love and gratitude that I thank my wife and children for your understanding and love during the past years. It is only with your support, encouragement, and perhaps most importantly, patience, that this dissertation possible. My parents also receive my deepest gratitude and love for their commitment to developing my work ethic, consistent, lifelong dedication to my education and the many years of support that provided the foundation for this work.

Last, but certainly not least, I thank my Lord God and His Son Jesus Christ, for all that I have and all that I am. Without You, I am nothing.

1 Introduction

This research develops an automatic method for locating and identifying landmarks in range scans. The identified landmarks are intrinsic to the model subject and are locally unique. The selection process requires no user interaction. This is an important capability, providing the means to organize, search, and compare 3-D scanned models. This research offers an efficient means of finding intrinsic landmarks in a range scan by using principal curvature values at range points.

Often, many scans of the same subject are available and there is a need to identify the subject by matching it with known models. Previous studies in automatic landmark detection have used pre-specified locations for detection. This research uses unique and view-invariant features to identify landmarks that characterize the underlying model. The presented method removes the requirement of having landmarks at fixed locations and allows the method to be applicable to any range scan. Landmarks are selected autonomously by the system from among key feature points that are identified across multiple models of the same object.

The objective of this research is to evaluate the effectiveness of intrinsic landmarks in characterizing models. As a novel approach to model characterization, the utility of intrinsic landmarks is unknown. By developing a method to select intrinsic landmarks and an evaluation technique to determine the validity of the selection, these concerns can be addressed. The objectives of this research are:

1. Given a set of range scans of a subject, select the same feature points in each scan of the subject.

2. Given a set of range scans of a subject and obtained feature points, select a number of stable landmarks specific to the subject.
3. Given a set of models, with a set of stable landmarks in each, identify new scans of those models.
4. Given a set of models, with a set of stable landmarks and known characteristics (i.e. gender, body mass index - BMI) in each, predict those characteristics in scans of new models with unknown characteristics.

The first two of these objectives address the selection of landmarks and generation of descriptors for them. The second two objectives are included in order to evaluate the effectiveness of intrinsic landmarks in the identification and characterization of models.

Several terms will be used consistently through this paper. Some of these terms and their definitions are as follows:

- Landmark: A point of interest on the model surface used to characterize that model. Often set at pre-specified locations determined by an external analysis of the model.

- Intrinsic Landmark: A landmark that is unique to the model subject and contains a descriptor of the local surface. They are selected from local surface properties, as opposed to pre-specified locations. Intrinsic landmarks are selected from feature points that occur across all scans of a subject.

- Feature Point: A point of interest on the model surface based on local principal curvatures. Feature points are potential intrinsic landmarks.

- Known model: A model that has been analyzed and had intrinsic landmarks selected.

2 Literature Review

Landmark identification in 3-D range scans has been the subject of many research programs. Over the past few decades, scanning technology has sufficiently progressed and the availability of high quality range scans has improved. As the quality and availability of range data has increased, so has interest in analyzing and utilizing it. However, this is a relatively new technology and a fully robust method for identifying landmarks is still in great demand. This research was developed based off a number of established techniques, with novel implementation and application toward landmark detection.

2.1 Relevant Techniques

The analysis of data consisting of large point clouds, such as the data used in this research, often requires the identification of one point's nearest neighbors. There are many techniques that have been used to identify such neighbors. Eppstein et al [**1**] write about the properties of nearest neighbor graphs. The information presented provides insight to the nature of nearest neighbor point clouds and some of the constraints and bounds that are likely to be encountered. In their paper, Sankaranarayanan et al [**2**], provide an algorithm to quickly identify nearest neighbors. The presented method uses the inherent locality of the neighborhoods to significantly reduce the time required for calculation.

The registration of one point cloud to another is an additional technique of interest. The registration of point clouds involves the definition of an affine transformation relating the clouds. Iterative Closest Point, or ICP, is a technique used for such registration. Williams et al [**3**] present a method that is incorporated into a generalized multi-view ICP surface matching system. In their implementation, a matrix is used to encode the point correspondence information and the

optimal solution is a result of an iterative process. Du et al [**4**] also build from the ICP technique. In this case, three constrained matrices are used to represent the affine transformation. These matrices are used to compose a quadratic programming problem. For optimal results, proper initial conditions and constraints are required.

Another technique that can be used for registering point clouds is the Random Sample Consensus, or RANSAC algorithm. This method is presented in the paper by Fischler et al [**5**] and discussed in a book section by Hartley et al [**6**]. The RANSAC method begins with a random matching of a small number of points from each cloud. The transformation parameters are calculated to relate these points to each other. This transformation is used on the remaining points and the number of points that are aligned is calculated. If there are not enough points aligned, new points are selected and the process is repeated. This continues until an adequate transformation is determined.

The notion of surface curvature is critical to this research. There are a variety of approaches that have been used to determine curvature values for surfaces. Peternell et al [**7**] provide an introduction to surface properties based on Laguerre geometry. The approximation of principal curvature values of folds is presented by Ozkaya [**8**]. In this method, a quadratic surface is fitted onto a structural surface in order to calculate the curvature values. Lange and Polthier [**9**] provide a method for determining curvature values of point cloud models that do not contain any mesh data. Using an anisotropic geometric mean curvature flow, a Laplacian shape operator is generated to find the curvature values. Harris [**10**] also uses a quadratic equation for surface representation. These equations are related to ellipsoids and are used in the derivation of curvature values.

Model data is generally stored as point clouds and triangular meshes. In order to conduct curvature analysis, smooth surfaces are necessary. The fitting of surfaces to point clouds is a well-studied subject. In a series of papers, Goshtasby address this subject [**11**,**12**,**13**]. The first paper introduces an algorithm that partitions a point cloud and fits a curve to each subset. The second paper presents a method to fit a parametric surface to a polygon mesh. This method creates a high level of continuity across the entire model and incorporates a smoothness parameter to adjust the desired resolution level. Finally, the third paper offers a new approach in surface definition. Here the surfaces are defined by a combination of control planes and gradient vectors, resulting in more flexibility than traditional formulations.

Various additional approaches for surface fitting can be found as well. Peternell [**14**] presents a method that defines a surface as envelopes of a one-parameter family of tangent planes. Nielson [**15**] offers an approximation method where the surface is defined implicitly as the level set of a field function which is a linear combination of trivariate radial basis functions. Kenobi et al [**16**] introduce the use of minimal geodesics through shaped data to produce low-order polynomials to represent the change in shape of the model. Finally, Flöry et al [**17**] attempt to reduce the impact of outliers by utilizing the I_1-norm as opposed to the I_2-norm, which is used in least squares optimizations, this is important due to the noisy nature of real world data.

Szeliski and Lavallée [**18**] offer a method for matching two surfaces. This method generates a non-rigid deformation between the surfaces, using octree-splines. In this case, the application is the medical field, where a modeled surface from a patient is compared to a desired reference surface. The approach represents the deformation using a combination of global polynomial deformations and local displacement splines. This is accomplished by the implementation of an

algorithm that minimizes the squared distances between the two surfaces using octree splines to improve the efficiency. This process avoids feature point identification and matching, which can be computationally intensive.

Human body models consist of several natural regions, or segments, including the torso, head, arms, and legs. It may be beneficial to analyze the segments separately. A method to automatically segment a human body model is presented by Zhong and Xu [**19**]. In this method, key characteristics of the human body are used for segmentation. The model point clouds are considered in the form of horizontal slices. Initial target zones are identified using generalized proportion information, i.e. – head length to body height. Working from these target zones, the segment boundaries are then determined from distance and angle changes between slices. Additional algorithms are implemented to confirm the validity of the segmentation and provide refinements if necessary. A different approach to segmentation is the identification of a model skeleton. Au et al [**20**] provide a method based on mesh contradiction, where the mesh geometry is first contracted into a zero volume skeletal shape. This shape is then converted and refined into a curve skeleton. This skeleton structure includes correspondence information, relating the mesh to the skeletal pieces. Using this approach, the model can then be segmented based on the limbs of the curve skeleton.

The role of feature point identification and scale determination is an important consideration examined by Lindeberg [**21**]. This research introduces potential methods to address the selection of appropriate scales, based on the data at hand, specifically feature points. It is asserted that an automatic scale selection method is essential for the automatic analysis of unknown model types.

2.2 Previous Landmark Detection in Models of Human Subjects

In 2001 Karla Simmons [**22**] conducted a thorough examination of Body Measurement Techniques available at that time. The report describes the uses and development of the hardware and measurement techniques. Three existing scanners were discussed, the Textile/Clothing Technology Corporation/Image Twin scanner, the Cyberware scanner, and the SYMCAD scanner. First the traditional anthropometry measurement techniques were described and compared to the measurement technique of the scanners. The author concluded that the three-dimensional scanners allowed measurements to be non-contact, instant, and accurate; however, she expressed concerns on the consistency of measurement methods across different systems. This report provided insight into the type of measurements needed for the textile industry and illustrated the early need for a consistent method for analyzing range data.

In 1999 the CAESAR (Civilian American and European Surface Anthropometry Resource) project was presented by Robinette et al [**23**]. She presents an early overview of the Air Force Research Laboratory's CAESAR project, between 1998 and 2001. This was a collaborative effort, led by the AFRL, with data collection and distribution by the Society of Automotive Engineers (SAE) in the United States and The Netherlands Organization for Applied Scientific Research (TNO) in Europe. Additionally, NISSAN, Magna Interiors, John Deere, Levis Strauss, Lear Seating and others collaborated on the project. The CAESAR results consisted of four different data sets, which are the following: demographic information, 40 traditional measurements with existing methods and 60 extracted from scans, 3-D coordinates for 72 pre-specified landmarks, and finally, complete 3-D scans in three postures. The traditional measurements were based on clothing and automotive industry standards. The pre-specified

landmarks were marked on the human body with physical markers, "flat" white discs when possible and 3-D boxes when the discs would not be visible. The three postures for the scans were: Standing – arms straight, but away from the body; Sitting, erect – arms out, hands up, at 90°, one grasping a dowel and one with fingers spread; Sitting, comfortable – hands on legs, natural position. At the time of the project, there was no fully automated landmark detection program that was robust and proven enough to be used; instead, manual landmark detection was planned. The original plan for detecting landmarks was presented later by Burnsides et al [**24**]. Initial efforts showed that manual detection could take up to 60 minutes per scan per subject. With several thousand subjects, the time required to mark the entire data set made a complete implementation unfeasible. This was not only because of the considerable time constraint, but also because of errors introduced when human fatigue sets in after hours of monotonous landmark identification work. An autonomous system was necessary to fully detect landmarks for thousands of scans.

The difficulties in locating landmarks and placing markers add to the complexity of model characterization. Not only are the landmarks of every individual varied in size and location, but the placement of the markers is subject to variance due to human tendencies. Kouchi and Mochimaru [**25**] specifically address these concerns in their study. In this study, 40 subjects had 35 landmarks marked by an expert and a novice marker. The markers by the expert were placed with invisible ink, viewable only under black light, in order to render the expert markers invisible to the novice. 34 body measurements were made, using both sets of markers, and the distance between landmark marker locations were also recorded. The results of the study indicate unacceptable errors in the identification of landmarks, where the placement of markers

was often outside of the region allowed by the industry standard, ISO 20685. It is suggested that improved landmark definitions be created and additional placement instructions developed.

An additional comparison of model characteristics to physically measured characteristics was conducted by Vuruskan et al [**26**]. In this study, the physical measurements of subjects were accomplished by experts and the same measurements were calculated by ScanWorX software[**27**]. This software calculates textile industry standard measurements on 3D body scans according to a robust rule set that is based on specific human body characteristics. The results of the study indicate a significant variation in the two measurements, where the software generated results generally calculated larger values. It is explained that the body position of scanned subjects is different from that of the positions traditionally used in garment measurement. In addition, it is noted that the scan data is limited to the surface of the model, which for regions such as the armpit area, a physical measurement could occur within body crevasses or from depressed regions of the subject, i.e. into the body fat or overlapping skin area.

Another early approach at generating information from human body models was presented by Dekker et al [**28**]. In this work, automated techniques were introduced to detect and label landmarks and then used to generate newly "skinned" models. These landmarks were identified manually according to rule based implementation of the ISO 8559 standard. Using these landmarks, the range points were segmented and refined to fit templates. These templates were then joined to create a smooth, continuous model. This model could then be adjusted to change characteristics of the model.

An additional study of feature extraction was conducted by Au and Yuen [**29**], considering only the torso. This approach uses a generic feature model of a mannequin. For each subject,

the scan model is aligned to the feature model by minimizing the distance between the points of the two models. A matching algorithm is implemented to associate the feature points of the scanned model to mannequin model. Using this alignment, the measurement difference between the mannequin and subject could be calculated in order to improve the fit of clothing.

Allen et al [**30**] provide a study of the human body shapes contained in the CAESAR data. The primary contribution is the fitting of high-resolution template mesh to the CAESAR scans, using the recorded landmark data. The CAESAR scans undergo refinement, including hole-filling and adjustment into a common parameterization. With the application of the template mesh to the parameterized models, new shapes can be produced to represent a variety of human body types, beyond that which is included in the CAESAR database. This is a valuable capability that retains the accuracy of modeling based off the scans of subjects, while providing the flexibility to create new models that vary in size, shape, ethnicity, etc.

A method to study 3-D range scans was presented by Wang et al [**31**,**32**]. The method detailed was not landmark identification, but instead parameterizations the 3-D range data to represent models. Recognizing the difficulty in processing large data sets, the authors devised a 3-step process to generate features of a model. First, a range data set was prepared, then a human model was constructed, and finally, feature of the model were extracted. The first step involved noise filtering and model orientation. In order to build the features, a model was first segmented into six parts, the head root, left and right arms, major body, and left and right legs. Each of these segments is cylindrical and is analyzed by slices. Meshes were created to fill holes using two parameters: membrane or thin plate energy minimized. This resulted in six fully covered segments. Finally, the features were extracted based on fuzzy logic using descriptors

such as: the chest being about ¾ of the height from side view. The descriptors were based on garment industry standards and were used to extract dimensions to characterize the segments. The method was efficient and preserved topology; however, in some cases the fuzzy rules selected incorrect body parts. Once the features were parameterized, new models were created without new scans by adjusting the parameters in the existing models.

An approach developed by Leong et al [**33**] used geometric properties and common proportions to describe a model. This approach did not use markers and identified 21 feature points and 35 feature lines based on geometric properties and common proportions of the human body. Similar to the previous method, a model was segmented into five major parts: arms, legs, and torso-and-head. Range data was encoded into a 2-D depth map to minimize data size and improve computational speed. The angle and height are used as image coordinates and the radius is represented in a 16-bit grey intensity. Laplace and Sobel masks were used to detect features, filtering noise and determining curve properties. The method was successful in detecting feature points and lines in the torso-and-head segment of 5 "standard" size female models.

Ben Azouz et al [**34**,**35**] at the National Research Council of Canada conducted numerous studies based off of the CAESAR database. The initial method required several steps; first was data processing which incorporated the following: the surface was smoothed using a Taubin filter, reoriented and segmented to remove the hands and feet, and partitioned into slices. The obtained model was placed in a cube of voxels, each of which is classified as either interior or exterior. The models were then converted to a vector with deviation vectors representing the difference in distances from the average. Eigenvectors of the matrix representing these deviation

vectors were used to define the model; with the first 40 eigenvectors spanning 92% of the variability. Each principal component was highly correlated to a body shape description.

This research was later expanded by Ben Azouz et al [**36**,**37**]. Using the volumetric representation and the eigenvectors, it was demonstrated that model variation could be created by altering the principal components. Furthermore, a landmark location method was implemented by inferencing over a pair-wise Markov random field. SPIN images [**38**] were used to characterize local surface features which were then matched to a best fit in the Markov random field. A set of 200 models were used to learn an initial loop belief. An additional 30 models were used to validate the method, obtaining encouraging results with some initial error.

The generation of anthropometric measurements is addressed by Wang et al [**39**]. This study introduces a method to use body scans to calculate measurements traditionally accomplished by hand. The models were examined by horizontal slices, and textile industry standard landmark locations were identified by visual examination. The anthropometric measurement values were then determined using algorithms based on the identified landmark locations.

Lu and Wang [**40**] expanded on the previous paper. This research is focused on the automated detection of landmarks in order to calculate known anthropometric measurements. The initial step requires segmentation based off of the generation of a 2D silhouette of the model. Textile industry standard landmark locations are then approximated according to generic proportion rules. Finally, additional algorithms incorporating minimum circumference determination, gray-scale detection, and human-body contour plots are applied to refine the

location of 12 landmarks. The location of these landmarks is used directly to calculate anthropometric measurements.

In a study of automatic landmark detection only on human torso models, Han et al [**41**] present an algorithm to accurately and automatically identify predefined landmarks. Using models acquired through the 5th Size Korea National Sizing Survey, detailed definitions were generated for five torso landmarks. The characteristics included maximum and minimum values, slope changes, silhouettes, and cross sections. Across a variety of specified body types, the landmark locations were visually identified, according to textile industry standards. Once identified, the characteristics were generated from the model data. These characteristics from each body type were compiled to create a representative characteristic for each landmark. Using these representative characteristics, in general, landmarks were very successfully located in new models. However, in some instances, due to the nature of human body shape variance, the identification of the physical landmark was not possible according to the standards. In these cases the method could not be expected to identify those landmarks.

An effort to improve the automated alignment of scanned models is presented by Hirshberg et al [**42**]. A model based approach was given that automatically aligns model meshes. An iterative closest point method was used to fit a low resolution template body mesh to each scanned model. A minimal set of initial landmark locations are identified in order to prevent the mesh from "slipping" and improve the fit. An analysis of the final template position and association of template to model mesh enabled the alignment and comparison of different model scans.

Siebert and Marshall [**43**] present an alternative method to scan subjects and create 3D models. This method generated photorealistic 3D models using speckle texture projection stereo-photogrammetry. The benefits of this method include the low cost of hardware and software, as the images are produced by standard cameras, and quasi-instantaneous capture. The approach relies on the projection of a known pattern onto the subject and photo capture of the subject via stereo cameras. The 3D models were then reconstructed based on the stereo images and knowledge of the pattern.

Another alternative method for generating scanned models is offered by Percoco [**44**]. This approach is similar to the previous method. This experimental scanner uses eight cameras and four image projectors. The method requires the subject to be coded, in this case through the wear of carefully patterned clothing. By aligning the photo images according to the clothing patterns, 3D model were reconstructed.

2.3 Related Work

The development of an automatic method for the selection of intrinsic landmarks has potential for use in variety of fields. For instance, the analysis of animal skulls for detection of speciation, environmental impacts and other effects often involve the identification of landmarks. Cardini et al [**45**] present an in-depth study of the skull structure of Vervet Monkeys. In this study, eighty-six landmarks were identified and characterized physically on 306 skulls. These were used as the basis for determining the differences in monkeys from a variety of regions and environments. Similarly, Tamlin et al [**46**] measure the features of physical skulls of wild and domestic minks in order to determine changes between the populations. For both of these studies, an automatic method for rapidly scanning these skulls and providing automatic selection

of landmarks could have enhanced the research; reducing the time spent conducting repetitive measurement and placements, while providing accessible and reusable models along with feature characteristics.

In a related application, intrinsic landmark selection could be used to aid in human facial recognition. The nature of human facial features is such that for every individual, the exact location and characteristics of each landmark will be different. Allowing intrinsic landmarks to select these key locations could lead to improved identification results. The research by Yin and Yourst [**47**] as well as Ghosh and Sinha [**48**] offer novel methods in the identification of individuals; these methods use a combination of photography and video to reconstruct facial models. The identification of facial landmarks is a critical piece of the facial reconstruction and could be improved by the application of intrinsic landmark selection.

3 Approach

With the increasing availability of range scans, it is critical to develop a method for sorting and comparing the scans. Existing methods have limitations. The methodology presented identifies unique intrinsic landmarks in the scans. Landmark selection is achieved by analyzing every range point and calculating its principal curvatures magnitude and direction and determining the average curvature of points in neighboring regions surrounding each landmark. Feature points are selected where the maximum principal curvature value is a local maximum or minimum and the minimum principal curvature value is a local maximum. Stable, intrinsic landmarks are selected from the feature points that are identified in all the scans of a subject based on a RANSAC (RANdom SAmple and Consensus) algorithm.

3.1 Landmarks

Landmarks are key, view-invariant feature points on the surface of a model. In a given set of models, consisting of range data on many different objects of the same type (i.e. – people, cars, skulls, etc.), each object would have distinct, uniquely characterized landmarks based on local shape characteristics. For example, a car type with a curved, smooth roof would have quite different landmarks than a car type that has sharp corners and edges. By identifying the location of these landmarks in every model, the cars could be sorted according to the number, location, and properties of the landmarks. Comparisons between cars could be made and new data could be identified as potentially matching one of the existing models, enabling meaningful analysis and study of the data.

3.2 Landmark Characterization

The identification and characterization of landmarks in a range scan is a non-trivial task. It is possible to visually locate landmarks on the models based on pre-specified definitions, such as the corners or center of the car roofs as mentioned previously. However, when there are numerous landmarks to find and thousands of models to find them in, the problem becomes intractable, due to time and accuracy constraints. It is also possible to pre-mark the landmarks on the subjects prior to scanning. However, this is also time-consuming and can be prone to error. These limitations can be overcome by designing a method that can automatically select landmarks on the range data.

In order to automatically select landmarks, it is necessary to establish a consistent method of characterization. The presented method examines each range point and considers its neighboring region. The critical values considered are the maximum and minimum principal curvatures. Given a three dimensional surface, at any point, there are two orthogonal principal curvature directions. The maximum and minimum curvature directions indicate the direction of the greatest and least curvature, respectively. Both directions lie on a plane tangent to the surface at the point and are therefore orthogonal to the surface normal. The magnitude of the curvature value represents how curved the surface is along that curvature direction. Consider Figure 1, Figure 2, and Figure 3, each showing the same surface. In these, the blue line represents the surface normal, purple, the maximum curvature direction and green, the minimum curvature direction. Figure 2 displays the surface as seen down the direction of minimum curvature, the direction of maximum curvature can be seen originating at the center of the image and continuing off to the left. Likewise, Figure 3 shows the surface as seen down the direction of

maximum curvature, the direction of minimum curvature can be seen originating at the center of the image continuing off to the right. It is important to remember that the principal curvature directions represent the direction of maximum and minimum curvature at that point on the surface; they are not curvature contour lines which represent continuous curves of maximum or minimum curvature along the surface.

Surface Normal **Maximum Curvature Direction** **Minimum Curvature Direction**

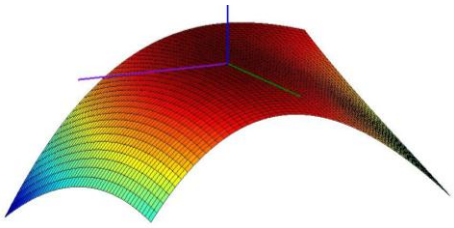

Figure 1 - Surface

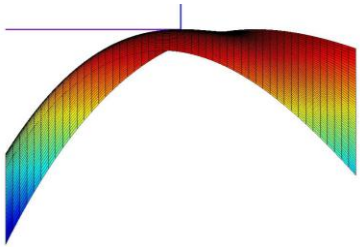

Figure 2 – Down minimum curvature direction

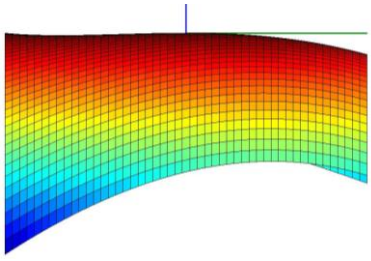

Figure 3 – Down maximum curvature direction

Once the principal curvatures and directions for every point are calculated, each point can then be characterized based on their own curvatures, as well as the curvatures of the points in neighboring regions. In Figure 4 a neighborhood of points is displayed, looking down the normal of the surface fitted to the neighborhood of points. Again, the green

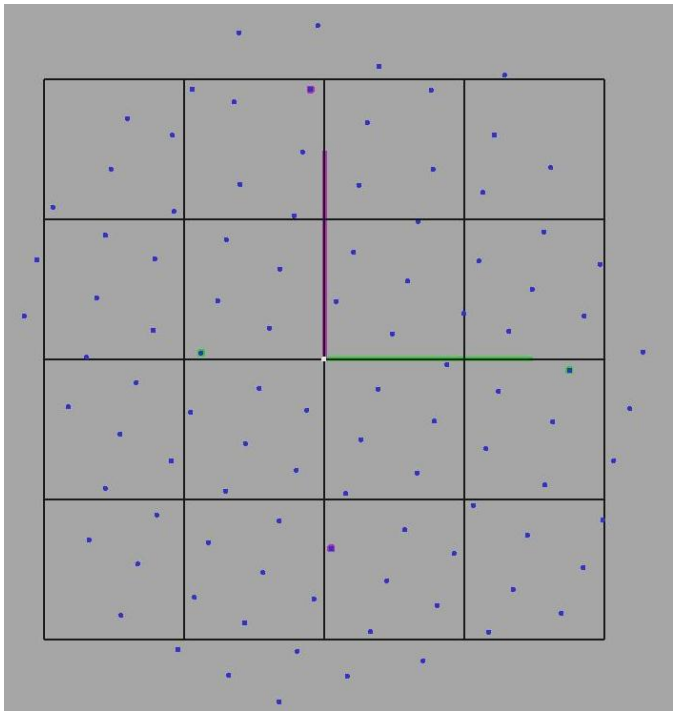

Figure 4 – Neighborhood with bins

line represents the direction of minimum curvature and the purple the direction of maximum curvature. This is important because the surface has been oriented based on the principal curvature directions, which allows the characterization to be invariant to rotation or model orientation. Regardless of the orientation of the point on the model, the direction of maximum curvature will be consistent. The points in the neighborhood are grouped into one of the 16 bins, which subdivide the region immediately surrounding the current point into preset, equal sized regions. With this arrangement, each point can be characterized based on 34 values, which include its own maximum and minimum principal curvature values as well as the average maximum and minimum principal curvature values of the points for each of the 16 bins. This characterization describes not only the attributes of the point itself, but that of the region surrounding it as well. In this way, landmarks can be distinctively identified. This characterization, based on the 34 principal curvature values provides a new and unique landmark descriptor.

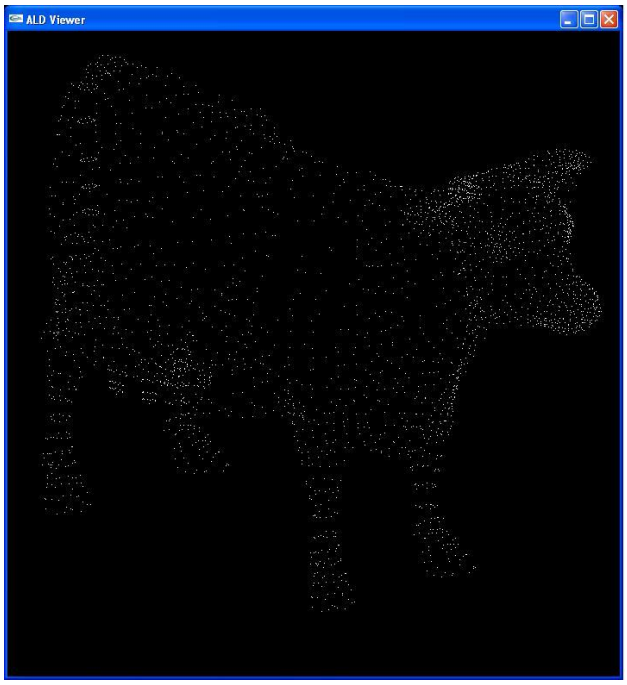

Figure 5 - Point cloud of cow

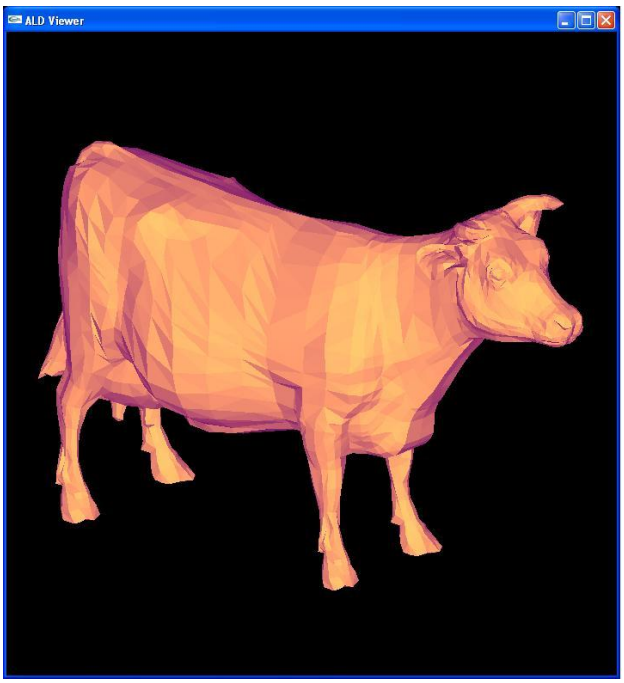

Figure 6 – Polygon mesh of cow

3.3 Characterizing a Landmark and its Neighborhood

To characterize a landmark, principal curvatures are calculated from an explicit function defining the surface surrounding the landmark. However model data is not stored as a smooth surface. In fact, the scanners generally generate a point cloud representing the surface of the subject. Software generates polygons (usually triangles) to connect the points and approximate the surface of the subject in the model with a polygon mesh. Figure 5 presents a point cloud generated to represent the shape of a cow. These points have been connected via triangles, as shown in Figure 6, in order to approximate to the shape of a cow. However, it clearly does not have smooth surfaces as expected on an actual cow and as required for principal curvature calculation. The point and polygon representation of a subject is an efficient method for data

storage and provides an approximate model for most uses. Certainly, a single explicit function could not be used to accurately define the shape of the subject. Nevertheless, an explicit function is necessary and can instead be calculated locally for each point. By examining all the connected points within a specified distance of the current point, a surface can be fitted and an explicit function defined. This surface will accurately represent the smooth shape surrounding the point and provide accurate principal curvature data for landmark characterization. The figures below display the fitting of a surface to a neighborhood of points and how it matches with the mesh.

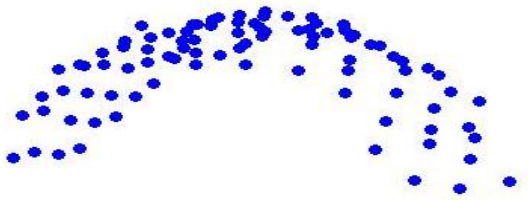

Figure 7 - Neighborhood point cloud

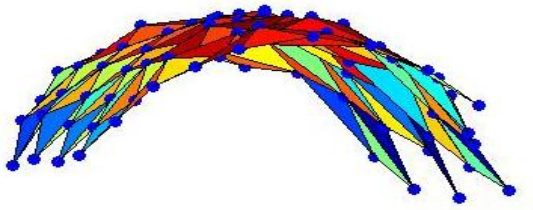

Figure 8 - Neighborhood points and mesh

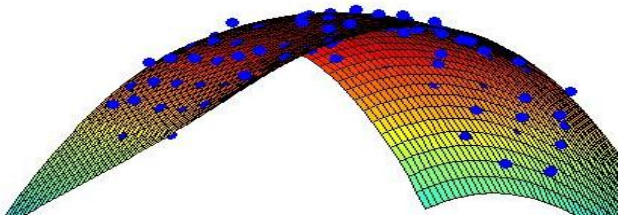

Figure 9 - Neighborhood points and surface

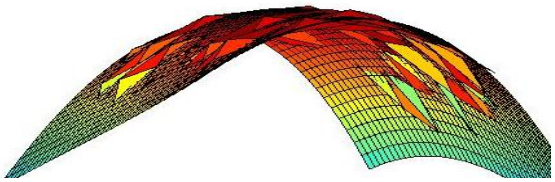

Figure 10 - Neighborhood mesh and surface

3.4 Model Data

This research uses model data from two sources. Both data sets were captured by the Air Force Research Laboratory for anthropometry studies. Robinette et al discuss the source of the first data set in their paper [**49**]. The purpose of this study was to investigate the accuracy of the 3-D body scanners. In order to conduct this investigation, twenty subjects were scanned by two

different research teams using two different scanners. The scanners were the Cyberware WB4 scanner and the Vitronic Viro 3D Pro scanner. Each subject was scanned three times in three different poses by both teams; the subjects were marked with white, circular disks at textile industry standard landmark locations. This set of scans for the twenty subjects is used as the basis for selecting intrinsic landmarks. The male models from the set are presented in Figure 11 and the female models in Figure 12. The second data set is the CAESAR set as discussed previously [**23**]. One hundred models were randomly selected from this set to evaluate the effectiveness of the intrinsic landmarks.

3.5 Assumptions and Constraints

In order to process the data in a timely and meaningful manner, some assumptions and constraints have been made. The raw model data has been selected due to availability and its comprehensive nature. This data is uniformly oriented and is rotated in preprocessing so that *x*, *y*, *z* axes align with the body's left-to-right width, front-to-back depth, and head-to-foot height respectively. This alignment is assumed in the data processing, however, it is reasonable to expect such an orientation and there are existing algorithms that could be used to preposition the models if necessary. Only the standing poses will be used in this stage of the research. Additional sets of landmarks could be selected for the other poses and likewise characterized. However, that is work for other projects and will not be addressed here.

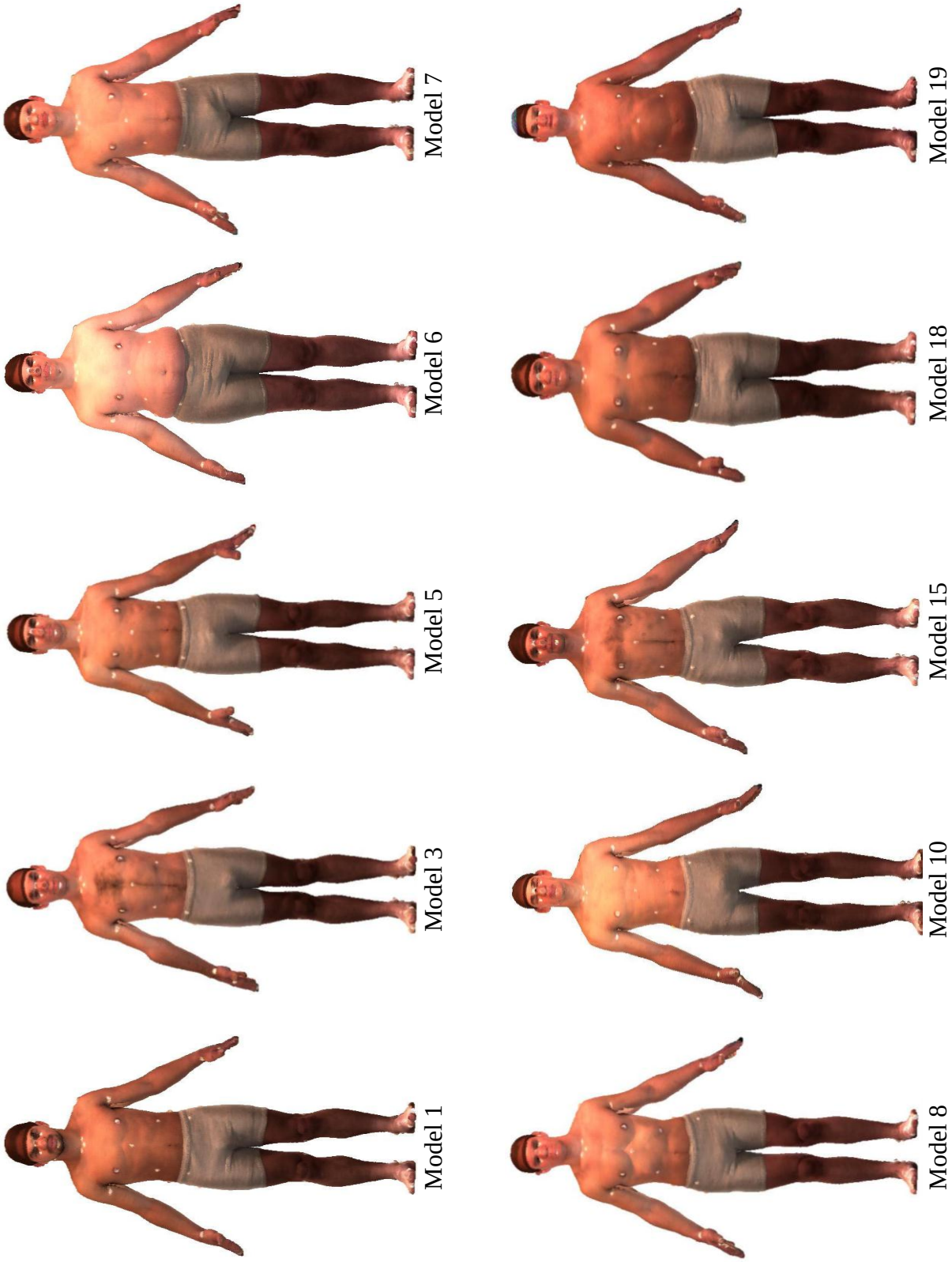

Figure 11 – Male Baseline Models

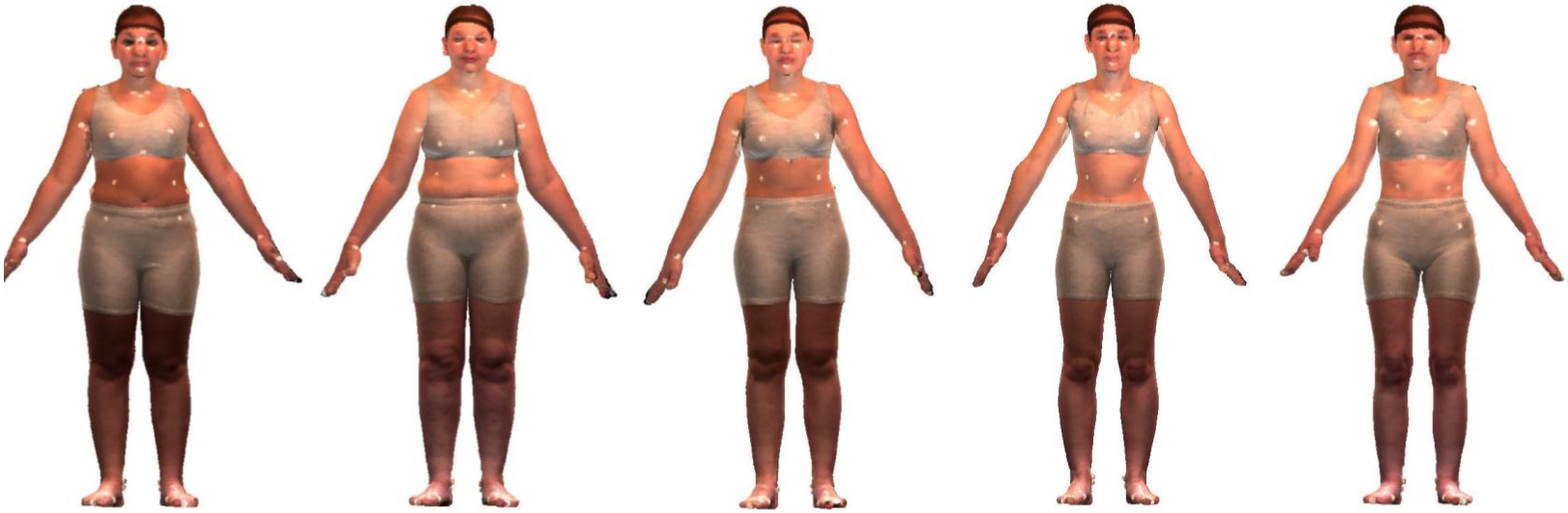

Model 2 Model 4 Model 9 Model 10 Model 12

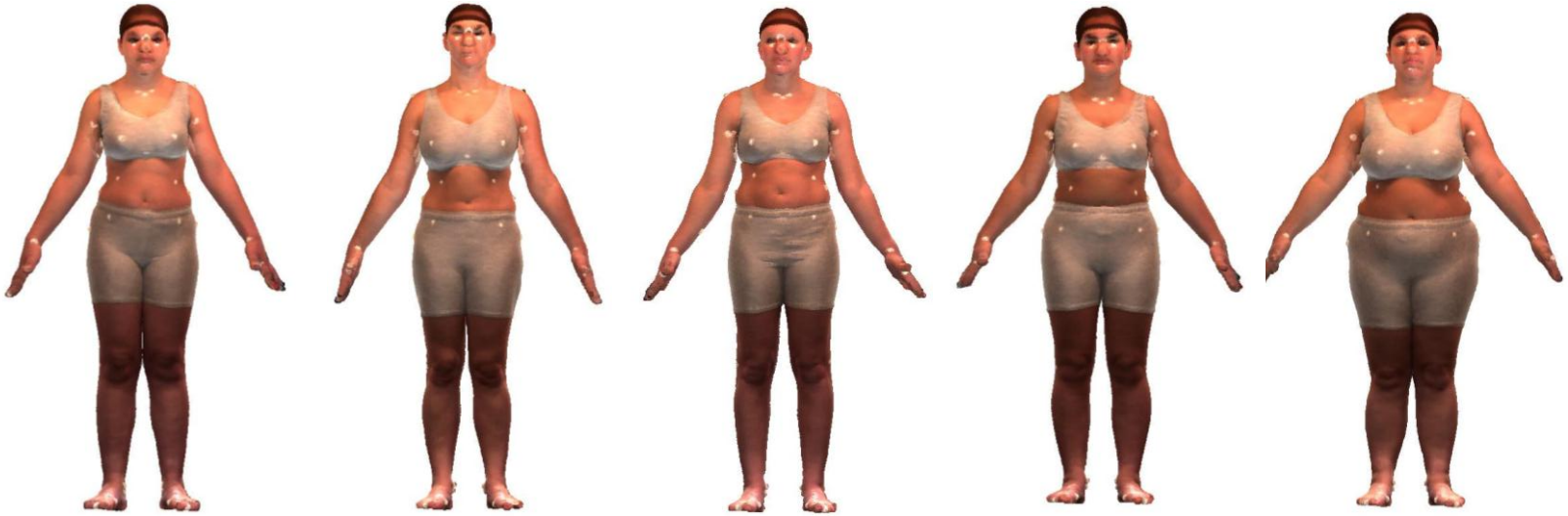

Model 13 Model 14 Model 16 Model 17 Model 18

Figure 12 - Female Baseline Models

4 Implementation

With an established landmark characterization, a methodology has been implemented to automatically select stable intrinsic landmarks in model data consisting of points and a triangle mesh. Incorporating an acceptable set of practical assumptions and constraints, range data is preprocessed prior to the automatic landmark selection process. Additionally, an evaluation method to determine the effectiveness of the selected landmarks was developed. The steps of this process and the following evaluation are presented along with the goals of the research that they address. The overall process for this research is summarized in Figure 13, a description and overview of each step follows.

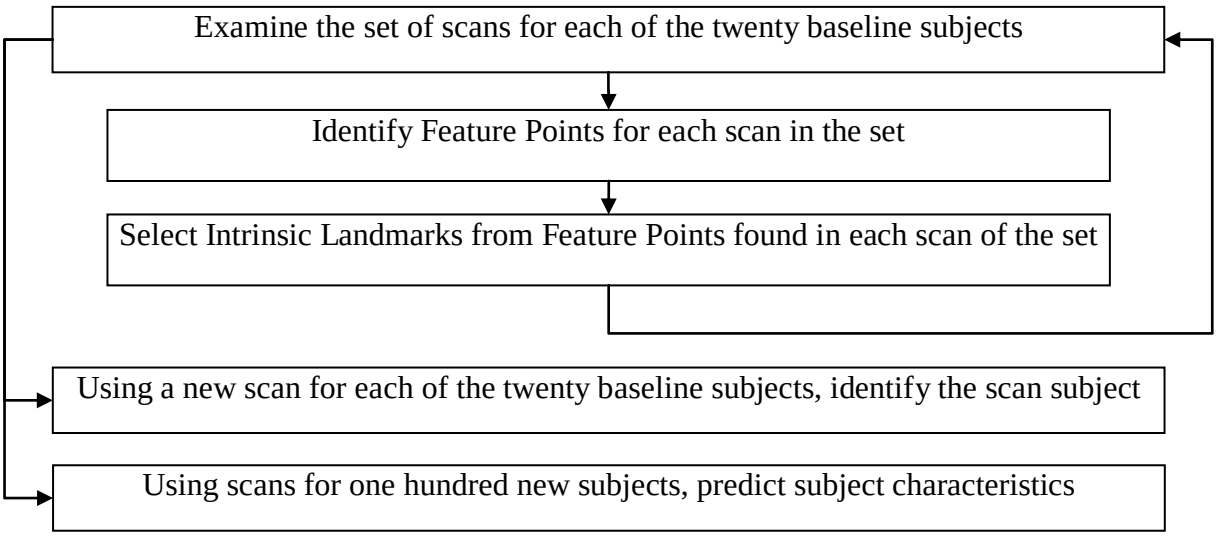

Figure 13 - Process Overview

1. Feature Point Generation: For each scan, every point will be examined and analyzed. Points with locally strong characteristics will be selected as feature points.

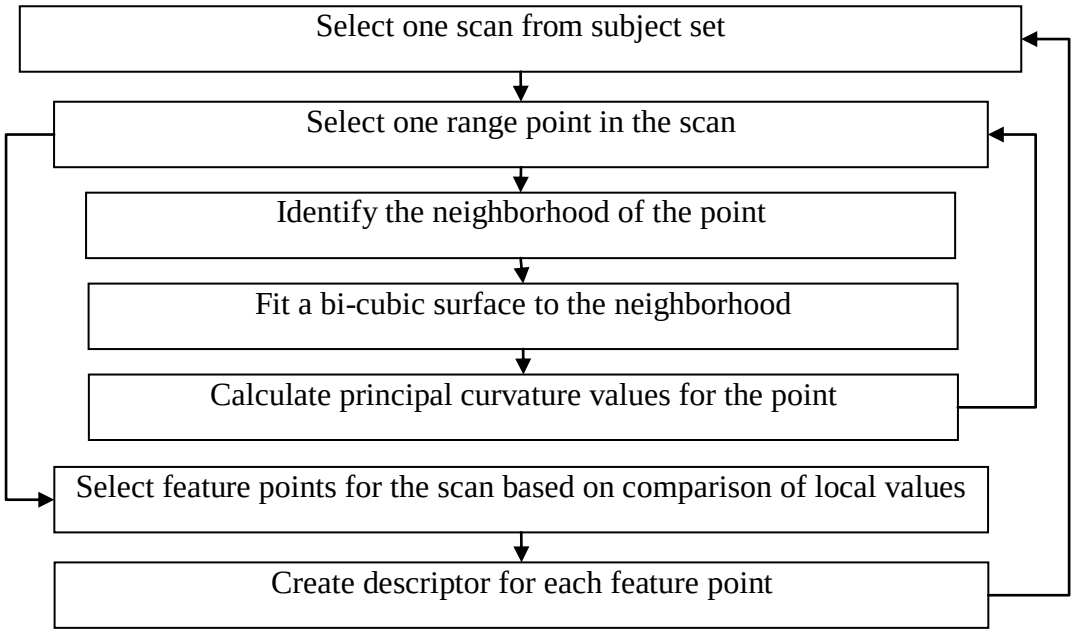

Figure 14 - Step 1 Overview

2. Intrinsic Landmark Selection: For each subject set, all six with feature points, stable intrinsic landmarks will be selected based on comparison using a RANSAC algorithm.

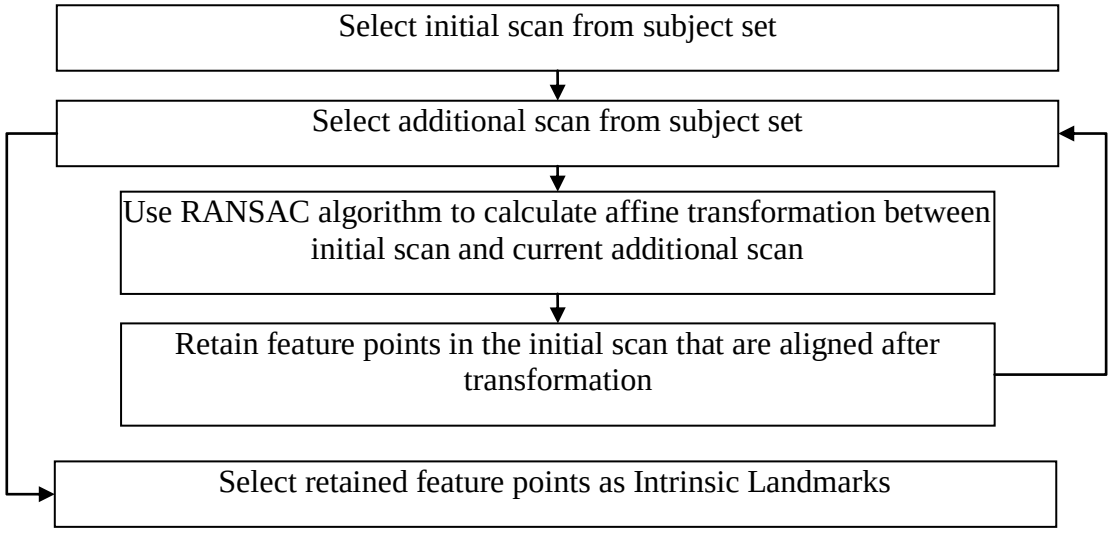

Figure 15 - Step 2 Overview

3. Known Model Identification: Stable Landmarks will be selected, using only five of the scans for each of the twenty models. The sixth scan of each model will then be compared and identified using intrinsic landmarks.

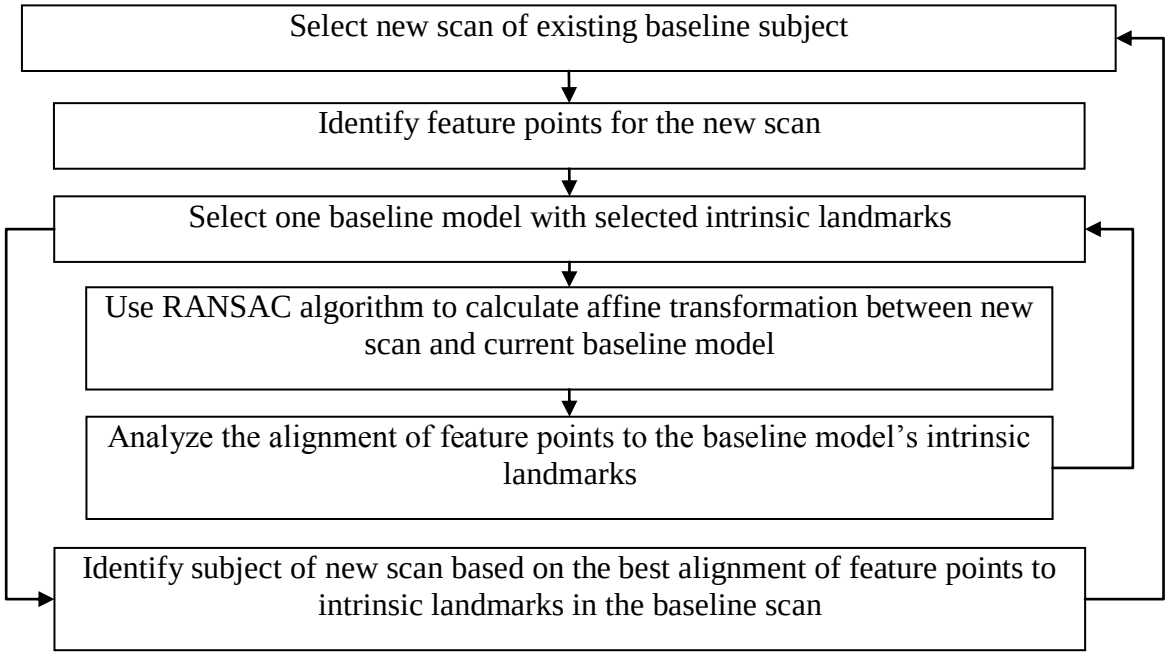

Figure 16 - Step 3 Overview

4. Model Characterization: Using the set of twenty subjects, with known characteristics, including gender and Body Mass Index (BMI), and selected intrinsic landmarks, these characteristics will be predicted for one hundred randomly selected CAESAR subject models.

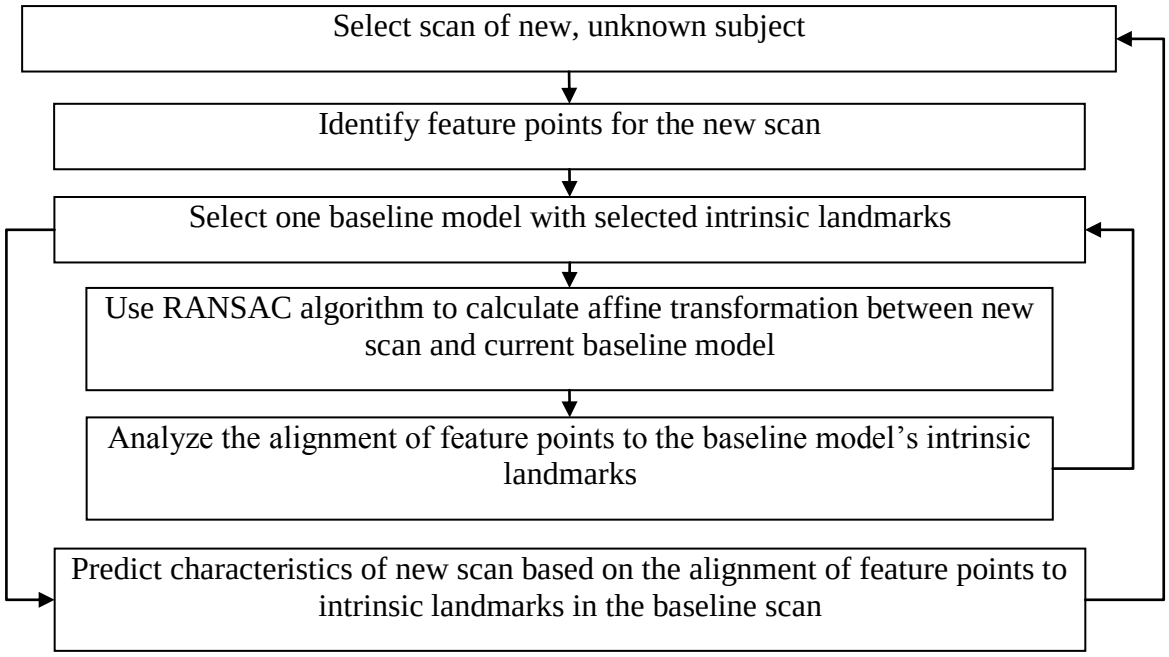

Figure 17 - Step 4 Overview

4.1 Feature Point Generation

In order to generate feature points for each scan, every point in the scan will be examined and analyzed. Points with locally strong characteristics will be selected as feature points. The generation of feature points is a multi-step process consisting of the following steps:

1. Identifying the neighborhood of the point currently under consideration.
2. Fitting of a bi-cubic surface to the neighborhood.
3. The selection of feature points based on the local strength of each point's principal curvature values.

4. The characterization of feature points; based on 34 total principal curvature values, including the maximum and minimum principal curvature of the point and its 16 surrounding regions.

The generation of feature points addresses the first objective, which was:

1. Given a set of range scans of a subject, select the same feature points in each scan of the subject.

4.1.1 Neighborhood Establishment

The first step of feature point generation is neighborhood selection. Examining each point in turn, a neighborhood of closest connected points is determined by searching along the surface of the model, selecting all connected points within a pre-specified radius of the current point. Using the triangle data, it is possible to select only connected points within the radius, avoiding those points that are close, but not connected by points within the radius. For instance, in a human model with arms down and close to the sides, it is necessary to exclude points from the torso when selecting the neighborhood of a point on the inner forearm. The points on the inner foreman and torso may be within the pre-specified radius; however it would not be appropriate to include the torso points when calculating the curvature of the inner forearm.

After selecting the neighborhood, it is translated so that the current point is at the origin. Because the principal curvature values are based only on local shape characteristics, the neighborhood can be examined in isolation from the rest of the model. This removes the impact from model rotation or orientation. The principal curvature directions lie on the surface tangent

plane at the current point under consideration, which is orthogonal to the surface normal. Because of this, the neighborhood is oriented such that the surface normal is along the *z*-axis, placing the principal curvature directions in the *x*-*y* plane. This is accomplished by first approximating the surface normal by fitting a plane through the current point and minimizing the distance of each point in the neighborhood to the plane using a linear least squares algorithm. Using the calculated function definition of the plane, its normal has two potential directions, opposite of one another. In order to ensure consistent comparison between different points in different models, it is critical that the surface normal points "out of" the model for all points. In this first step of orientation, "out of" the model is assumed to be away from the center of the model. This will be accurate for most points, for others (such as the inner forearm), the direction will be corrected later. The plane normal direction that maximizes the dot product with a vector from the center of the model is selected. Here, the center of the model has undergone the same translation as the neighborhood. Once the direction of the plane normal has been determined, the the neighborhood is rotated such that the plane normal is now on the *z*-axis.

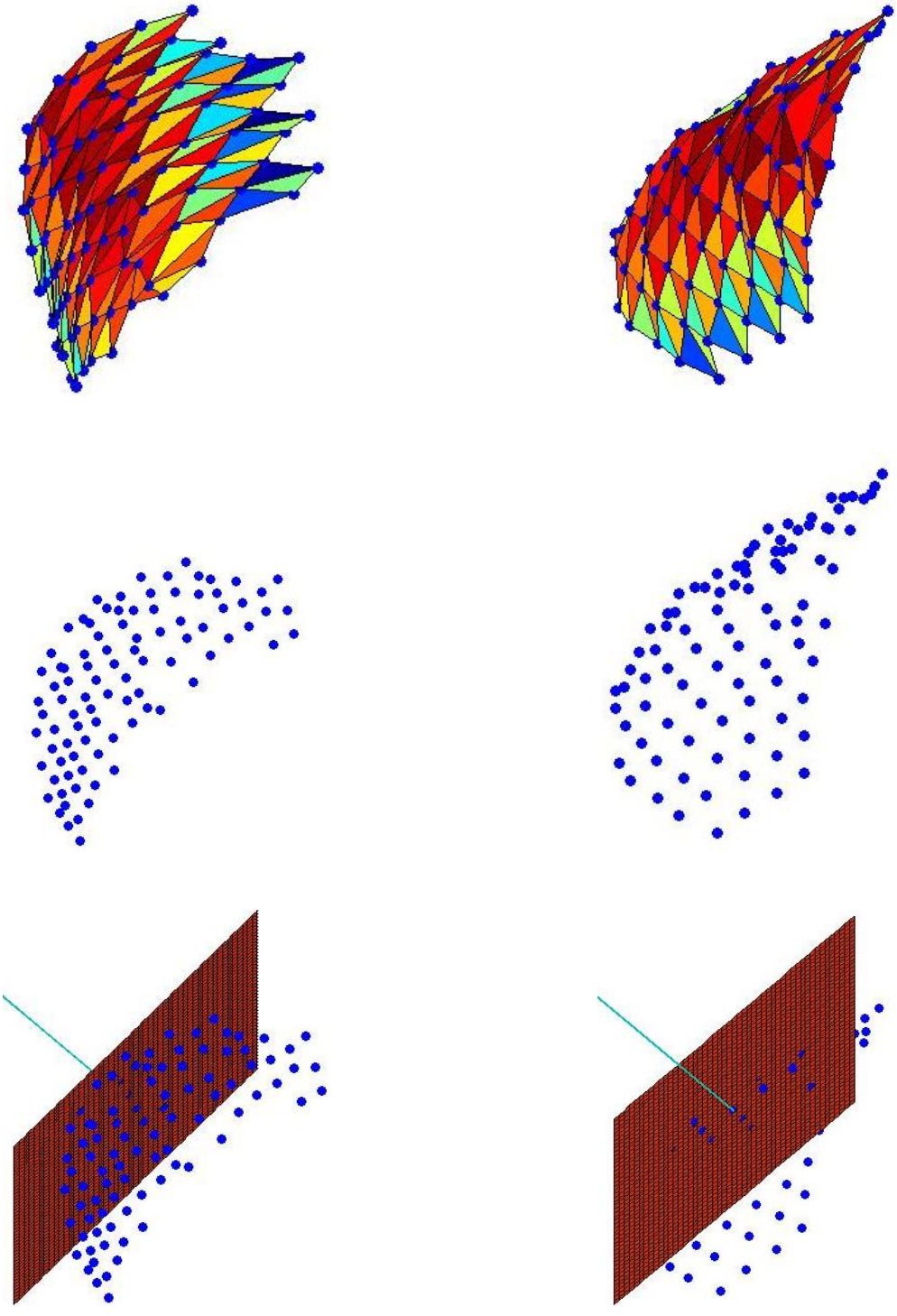

Figure 18 - A neighborhood from two different points of view

Figure 18 displays a neighborhood from two different points of view. The top images present the local neighborhood with the range points and triangular mesh. The middle images are of the neighborhood point cloud only. The bottom graphics show the fitted plane and plane normal. The same neigborhood is displayed in Figure 19, where the fitted plane is the horizontal line in the center of the graphics and the plane normal is shown aligned with the *z*-axis.

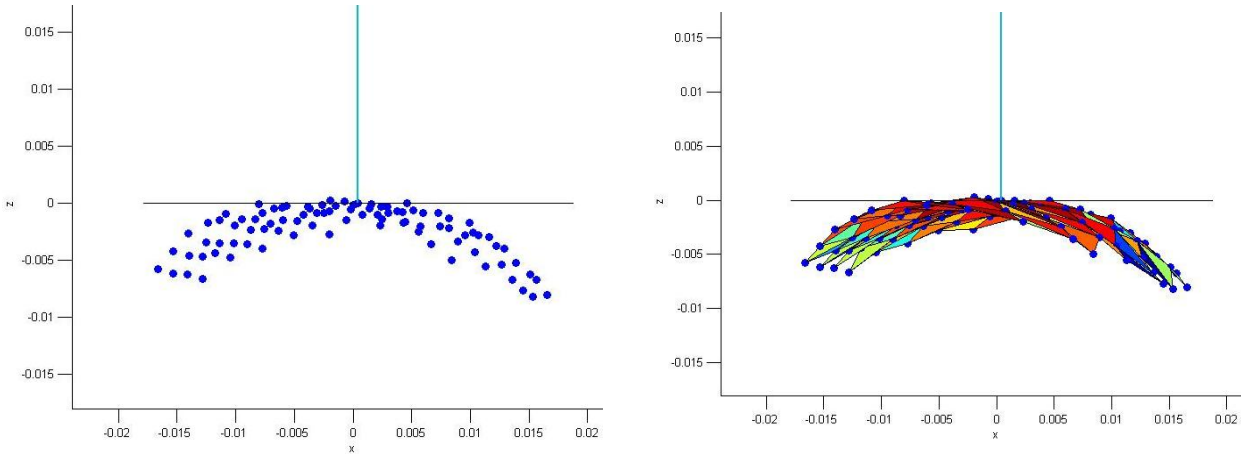

Figure 19 - Aligned neighborhood

4.1.2 Surface Fitting

After the neighborhood has been properly oriented, an explicit function can be calculated to fit a surface to the points. The explicit function is defined by the following bi-cubic polynomial:

$$f(x,y) = \sum_{i=0}^{3}\sum_{j=0}^{3} a_{ij} x^i y^j \tag{1}$$

The coefficients of the polynomial are determined using a weighted least squares algorithm to minimize the distance between the calculated *f(x, y)* and actual *z* value for each neighboring point, with the points closer to the origin given a greater weight. Given this definition of the

surface, the actual surface normal direction can be computed. Once again the neighborhood and surface are rotated such that the true surface normal is along the *z*-axis.

Figure 20 displays a local neighborhood from two points of view and the polynomial surface fitted to it. From top to bottom, the image presents the: range points and triangular mesh, point cloud, point cloud and fitted polynomial, triangular mesh and fitted polynomial, and finally, the polynomial surface. The fitted surface matches the mesh very closely, while presenting a smoother surface, as expected. This neighborhood is taken from the forearm of a human model in the CAESAR data set and the actual surface calculated to fit it.

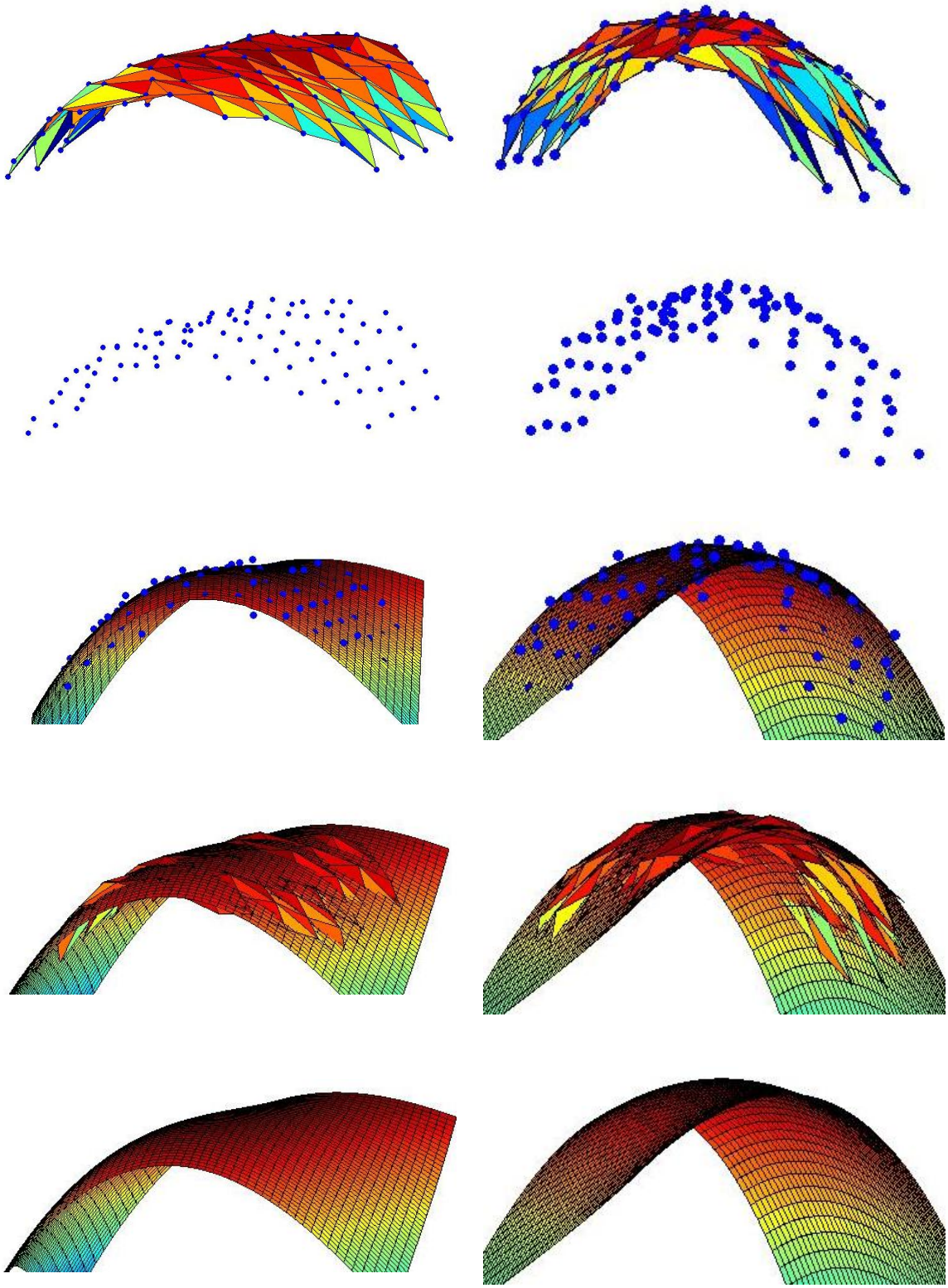

Figure 20 - Polynomial fitted to neighborhood

With the explicit function defining the local surface, the principal curvatures and directions can be determined directly as follows [**50**]. These equations are based on the *first* and *second fundamental forms* of a unique surface. These forms require a parameterization of the surface. Using the following parameterization:

$$\mathbf{p}(u,w) = [u, w, f(u,w)] \tag{2}$$

where, *u* corresponds to *x*, *w* to *y*, and *f* to *z*, such that:

$$f(u,w) = au^3 + bu^2w + cuw^2 + dw^3 + eu^2 + fuw + gw^2 + hu + iw + j \tag{3}$$

The first form is I:

$$d\mathbf{p}\cdot d\mathbf{p} = Edu^2 + 2Fdudw + Gdw^2 \tag{4}$$

and the coefficients can be calculated:

$$E = \boldsymbol{p}^u \cdot \boldsymbol{p}^u \tag{5}$$

$$F = \boldsymbol{p}^u \cdot \boldsymbol{p}^w \tag{6}$$

$$G = \boldsymbol{p}^{\mathbf{w}} \cdot \boldsymbol{p}^w| \tag{7}$$

Based on this parameterization, with simplification, the coefficients become:

$$E = 1 + (3au^2 + 2buw + cw^2 + 2eu + fw + h)^2 \tag{8}$$

$$F = (3au^2 + 2buw + cw^2 + 2eu + fw + h) * (bu^2 + 2cuw + 3dw^2 + fu + 2gw + i) \tag{9}$$

$$G = 1 + (bu^2 + 2cuw + 3dw^2 + fu + 2gw + i)^2 \tag{10}$$

However, when the surface is fitted at the origin, $u = 0$ and $w = 0$, and the coefficients reduce to:

$$E|_{u=0,w=0} = 1 + h^2 \tag{11}$$

$$F|_{u=0,w=0} = hi \tag{12}$$

$$G|_{u=0,w=0} = 1 + i^2 \tag{13}$$

Likewise, the second form is II:

$$-d\mathbf{p}(u,w) \cdot d\mathbf{n}(u,w) = Ldu^2 + 2Mdudw + Ndw^2 \tag{14}$$

and its coefficients can be calculated:

$$L = \mathbf{p}^{\mathrm{uu}} \cdot \mathbf{n} \tag{15}$$

$$M = \mathbf{p}^{\mathrm{uw}} \cdot \mathbf{n} \tag{16}$$

$$N = \mathbf{p}^{\mathrm{ww}} \cdot \mathbf{n} \tag{17}$$

where:

$$\mathbf{n} = \frac{\mathbf{p}^u \times \mathbf{p}^w}{|\mathbf{p}^u \times \mathbf{p}^w|} \tag{17}$$

Once again, with simplification and reduction for $u = 0$ and $w = 0$, we have:

$$L|_{u=0,w=0} = \frac{2e}{\sqrt{1+i^2+h^2}} \tag{18}$$

$$M|_{u=0,w=0} = \frac{f}{\sqrt{1+i^2+h^2}} \tag{19}$$

$$N|_{u=0,w=0} = \frac{2g}{\sqrt{1+i^2+h^2}} \tag{20}$$

With these coefficients, the principal curvatures can be calculated by solving the following equation:

$$(EG - F^2)\varkappa^2 - (En + GL - 2FM)\varkappa + (LN - M^2) = 0 \tag{21}$$

Where the roots of this equation are the principal curvature values. Figure 21 displays color maps of these principal curvature values on a human model. Areas of low magnitude curvature are "average" blue, lighter blue represents areas of larger positive curvature and darker blue represents areas of larger negative curvature. The minimum curvature color map consists of primarily "average" blue areas because, for most of the human body, the surface is relatively flat in the direction of least curvature. Areas such as the nose, finger tips, and toes all have a high negative curvature in the minimum principal curvature direction because they are rounded in all curvature directions.

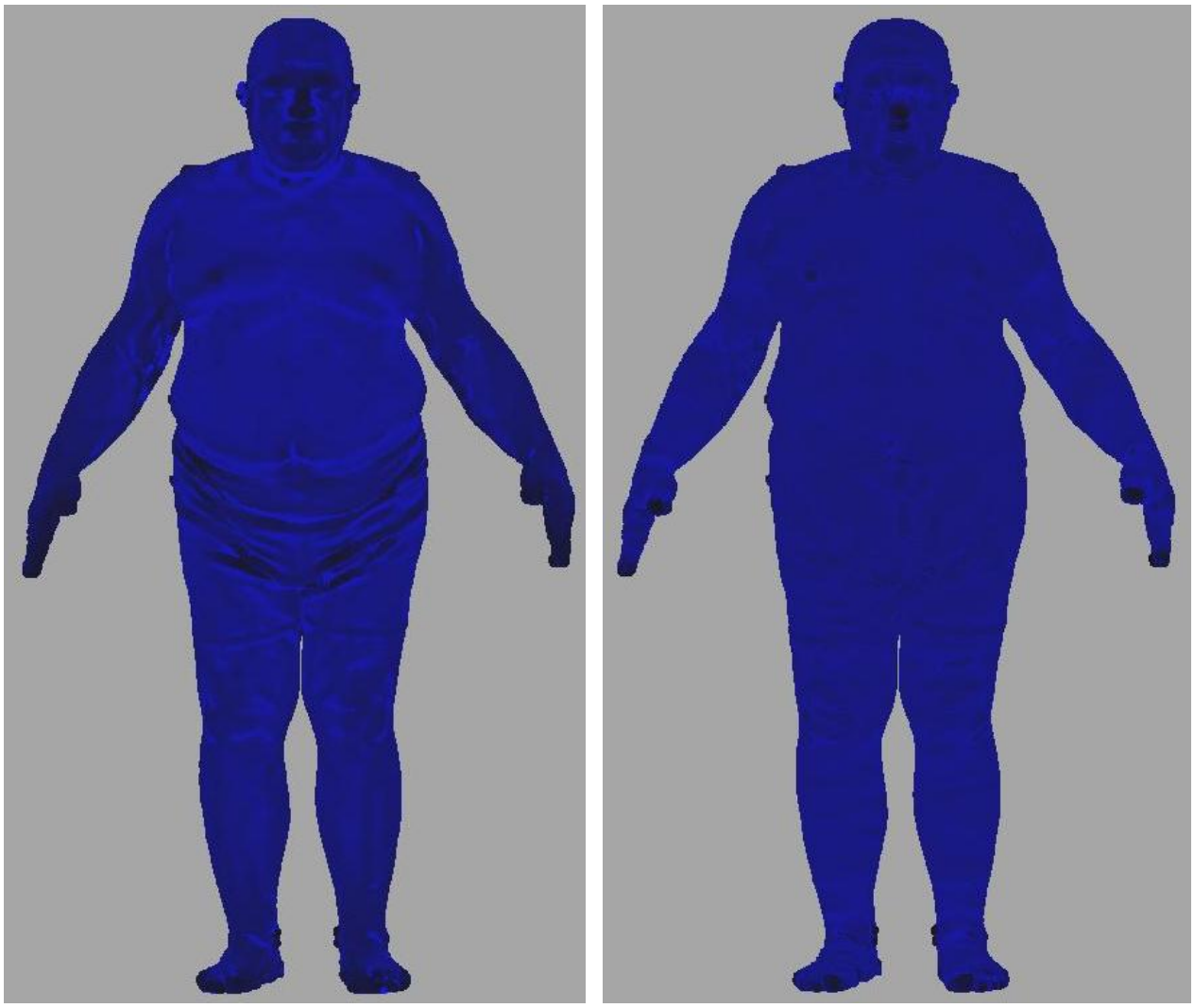

Figure 21 - Curvature color maps, left is maximum curvature and right is minimum curvature

The principal directions can be found, by considering $h = dw/du$ and solving this quadratic equation:

$$(FN - GM)h^2 + (EN - GL)h + (EM - FL) = 0 \quad (22)$$

Here the roots represent the ratio in the *dw/du* (or *y/x*) plane between the curvature directions.

So, the curvature directions are:

$$curvDir_1 = [h_1, 1, 0] \tag{23}$$

$$curvDir_2 = [h_2, 1, 0] \tag{24}$$

Figure 22 presents a fitted surface with the calculated principal curvature directions displayed.

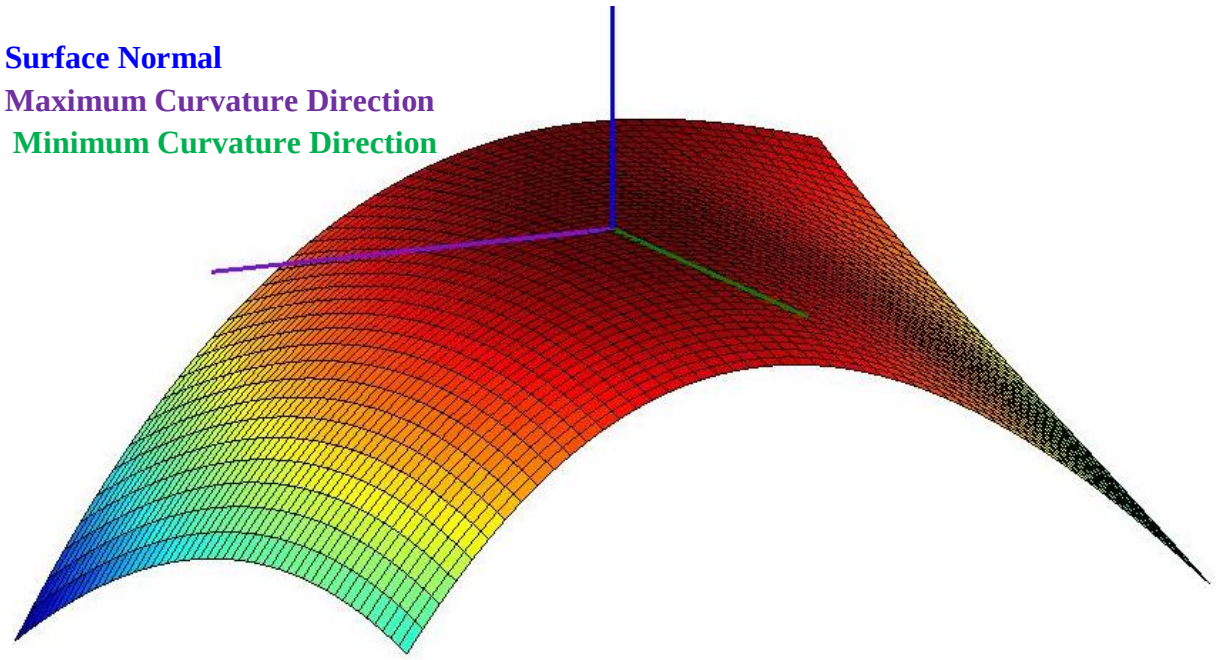

Figure 22 - Fitted surface

After determining the principal curvature directions, the neighborhood must be reoriented so that the maximum curvature direction is on the *x* axis and the minimum curvature direction is on the *y* axis. By aligning the principal curvature directions to the *x* and *y* axes, the shape (based on curvature values) of the region surrounding the point can be consistently compared to the shape of other points. Since the neighborhood is examined in isolation from the model, this alignment assures that there is uniformity in the orientation of neighborhoods under comparison. The principal curvature directions found are not explicitly associated with the maximum or minimum

direction. The proper association is determined by checking every point in the neighborhood to find a point closest to the positive and negative axis of each curvature direction. Based on the average slope of change for the *z* value of the two points on each axis, the maximum curvature direction is selected as the axis with the largest *z* slope, representing the greatest curve.

Because some of the selected normal directions may point "into" the model, the direction of the surface normal must be stored for future use and possible correction. This direction must be stored according to the reference frame of the entire model. Taking the surface normal (now along the *z* axis) and reversing all the rotations of the neighborhood provides the surface normal direction at the point with reference to the model. This reverse rotation is accomplished by applying the inverse of the rotation matrix, which must be calculated and stored with each rotation. Because it is an orthogonal matrix, the inverse can be found by transposing the rotation matrix.

Finally, each point in the neighborhood must be associated to one of the bins subdividing the region. As seen in Figure 23, the neighborhood is divided around the current point (at the origin) into 16 equal sized, square bins, via a 4x4 grid in the *x/y* plane. The width of each bin is 2/5 of the neighborhood radius. Because the neighborhood points are selected according to this radius, the neighborhoods tend to be circular in nature. If the bin size was set at half the radius, the corner bins would not be as populated as the center bins. In order to fully populate all the bins, the size is set to a value less than half of the radius, leaving several points in each neighborhood outside of a bin, but more fully populating all bins. Each neighborhood point is assigned a bin according to its *x* and *y* coordinates. If the point falls outside of the bin region, it is assigned to a null bin.

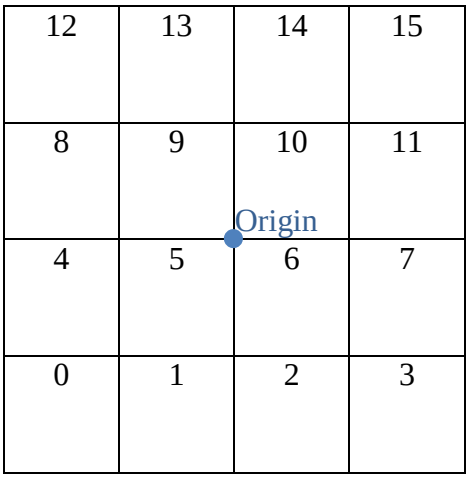

Figure 23 - Neighborhood bins

4.1.3 Feature Point Selection

Feature points are selected by examining each point. The maximum principle curvature of that point is checked against the maximum principle curvatures of its neighbors. The examined point is marked as a local maximum, local minimum, or neither for the maximum principle curvature. Likewise, the examined point is labeled based on its minimum principle curvature. Finally, the examined point is considered to be a feature point if its maximum principle curvature is either a local maximum or minimum and its minimum principle curvature is a local maximum.

4.1.4 Feature Point Characterization

After calculating the principal curvature values and surface normal direction for every point in the model, the definitive normal direction can be determined and the region surround each feature point characterized. In order to determine the definitive normal direction, every point must be reconciled with the points surrounding it, ensuring consistency. Starting with an extreme point on the model, for instance the top of the head for a human model, assume the neighborhood is oriented correctly. This is a sound assumption, because for an extreme point,

the direction pointing away from the model must be the same as direction pointing away from the center of the model, which is the default direction selected for the surface normal. With the normal direction of a single point confirmed, the normal direction of nearby surrounding points can be confirmed by checking the dot products of the two normal vectors. Points with normal directions nearly opposite have their normal vectors and curvature values flipped, by multiplying by a -1. Bin assignments are changed as well, to reflect the flip of the neighborhood. Figure 24 displays points on a human model that have been flipped due to disagreement in the direction of normal vectors. As expected, regions facing toward the center of the model required flipping, as seen in red. Agreement between principal curvature axes direction can be confirmed in a similar manner.

Once consistency of orientation has been established throughout the model, each feature point can be fully characterized. For all of the sixteen bins surrounding the point, points outside of the bins (bin number -1) are ignored; the average maximum and minimum principal curvature are calculated within each bin and stored in an array. The figures below display a fully oriented and characterized neighborhood. The blue points have the original *x, y, z* coordinates from the model and the orange points have *z* values based on the fitted surface function. The blue line is the surface normal, the green line the direction of maximum curvature, and the purple line the direction of minimum curvature.

Figure 24 - Flipped points

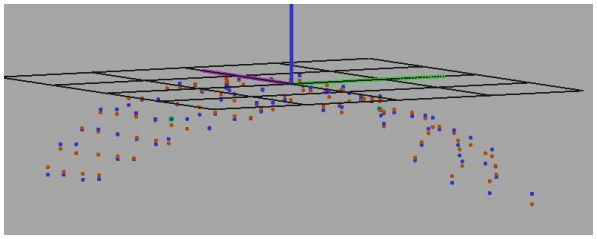

Figure 25 - Fitted neighborhood

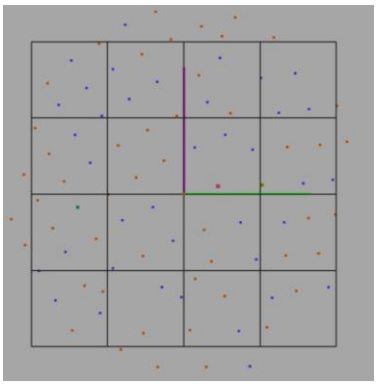

Figure 26 - Neighborhood bins

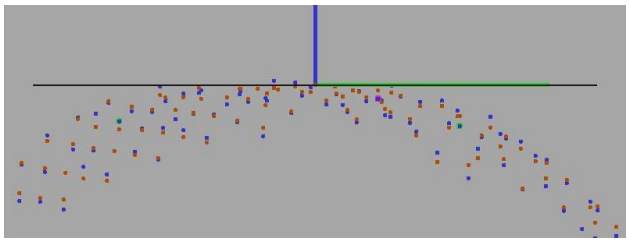

Figure 27 - Neighborhood down direction of minimum curvature

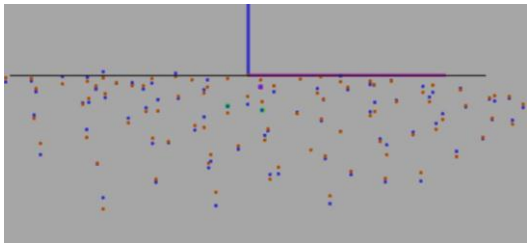

Figure 28 - Neighborhood down direction of maximum curvature

4.1.5 Feature Point Selection Summary

Figure 29 and Figure 30 present the selected feature points from two models, one male and one female. A visual examination of the feature points across models offers encouraging feedback concerning the goal of selecting the same feature points across all scans of a subject. Feature point selection was designed such that a large number of points were selected; for these subjects, several thousand feature points have been selected, from the over one hundred thousand range points. While it appears from the images that there is considerable overlap in selected points between the scans, this will not be confirmed until the Landmark Selection process is accomplished.

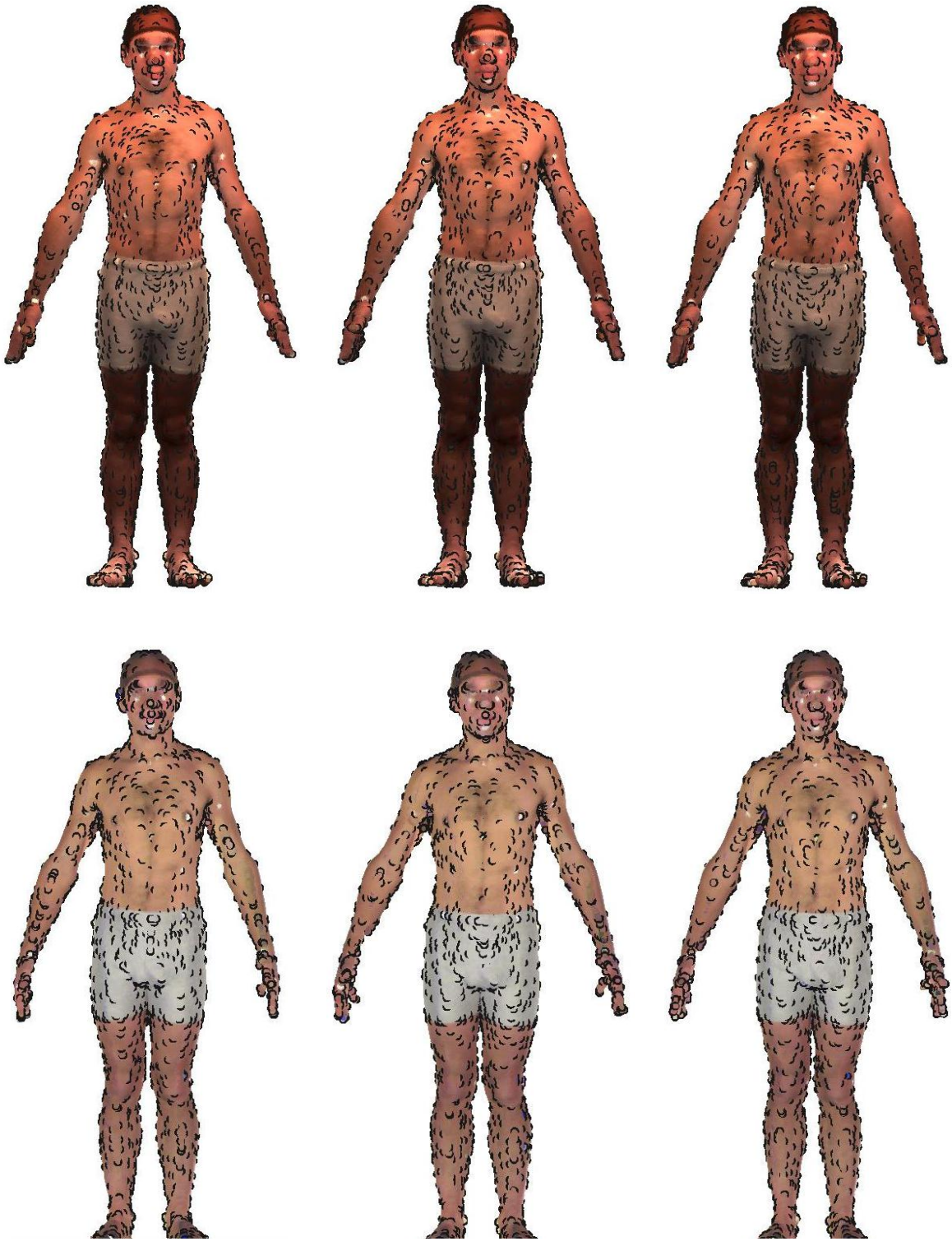

Figure 29 - Selected feature points on male subject, six different scans

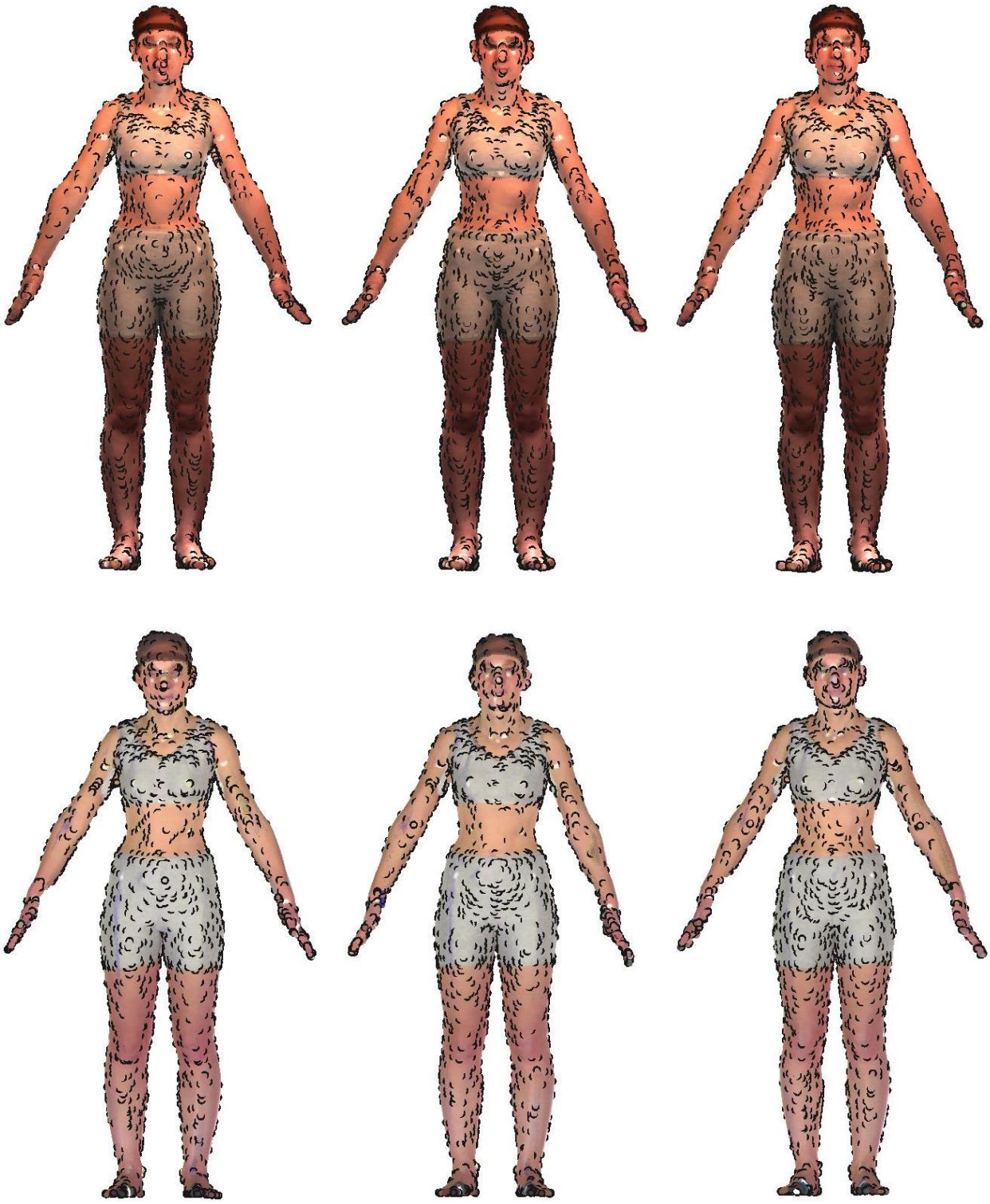

Figure 30 - Selected feature points on female subject, six different scans

4.2 Intrinsic Landmark Selection

After generating fully characterized feature points for each scan of every model, stable intrinsic landmarks were selected. This addresses the second objective of this research:

2. Given a set of range scans of a subject, with feature points, select a number of stable landmarks specific to the subject.

In the selection of intrinsic landmarks, the realization of the first objective was checked. If there were sufficient matched feature points across all models, then there would be sufficient stable landmarks, which, with the data used, should be several hundred selected landmarks, from the several thousand feature points.

The landmark selection method consisted of an iterative process that refined the set of feature points, until only the stable landmarks remain. During the process, one scan was compared to the other scans from the same subject. Based on a RANSAC algorithm [**6**], an affine transformation relating the two scans was calculated. Feature points that were aligned following the transformation were retained, unmatched feature points were discarded. The process was repeated for each of the additional scans; with weaker feature points discarded each step. Feature points remaining after all scans of the subject had been considered were selected as intrinsic landmarks

4.2.1 Transformation Calculation

After generating the feature points for all scans of each subject, the first step in selecting stable intrinsic landmarks was to consider one of those scans. This scan was the baseline and the feature points associated with it were reduced to the stable landmarks. A RANSAC algorithm

was utilized to define a transformation relating two of the scanned models. An affine transformation was used to approximate a rigid transformation, allowing for some deformation. It was defined by the following equations, where (x_i, y_i, z_i) is the coordinates of the points in the second model and (X_i, Y_i, Z_i) is the coordinates of those points transformed to the coordinate system of the first model:

$$X_i = ax_i + by_i + cz_i + d \tag{25}$$

$$Y_i = ex_i + fy_i + gz_i + h \tag{26}$$

$$Z_i = jx_i + ky_i + lz_i + m \tag{27}$$

A set of four feature points were selected from the second model. Four points were required in order to determine the 12 unknown coefficients of the affine transformation. These selected points were matched to feature points in the other model, based on the similarity of the 34 curvature characteristics of the two points and general agreement in direction. The coefficients of the affine transformation were calculated, mapping the coordinates of the second model to that of the first, by linear least squares.

4.2.2 Transformation Evaluation

Once the coefficients of the transformation equations had been determined, the unmatched feature points were transformed from the coordinate system of the second model to that of the first. For each transformed feature point, a check was made to determine whether there was a feature point within a distance ε (3.5 *cm*), in the first model's coordinate system. When that was the case, the points were considered matching. If at least 85% of the feature points matched, then the transformation was considered valid and RANSAC was considered complete. However,

if there were not enough matching feature points, the previous steps were repeated, with a new set of 4 points from the second model. This is continued until at least 85% of the feature points matched.

4.2.3 Feature Point Reduction

With a valid transformation between the two models, the feature points of the two models were further compared. In order to select the most stable landmarks, the search distance, ε, as reduced and feature points were required to match more closely, or be discarded. The feature points from the first model that had a closely matched transformed feature point from the second model were retained as potential intrinsic landmarks.

4.2.4 Landmark Selection

After reducing the number of feature points in the first model, based on matches to the second model, another model was selected for comparison. The previous steps were repeated, however, the set of feature points in the first model were the reduced set. This continued until every scan of the subject had been considered. With each additional scan, the number of potential landmarks decreased. The expectation was that the number of retained potential landmarks would approach a plateau, representing the model's stable, intrinsic landmarks. After every scan of the model had been considered, the remaining feature points were used to select the intrinsic landmarks.

4.2.5 Landmark Refining

After all scans had been considered, the number of feature points was reduced to include only those matched across each scans. The actual definition of the intrinsic landmarks required a further step. First the descriptor of the intrinsic landmark was determined. This was

accomplished by averaging the descriptor for the matched landmarks from each scan, resulting in the definitive descriptor of the landmark. Then the coordinates for all matched feature points were transformed to a single coordinate system. The centroid of each set was computed, representing the average location of the matched feature points. The coordinates of this location were selected as the coordinates of the stable intrinsic landmark.

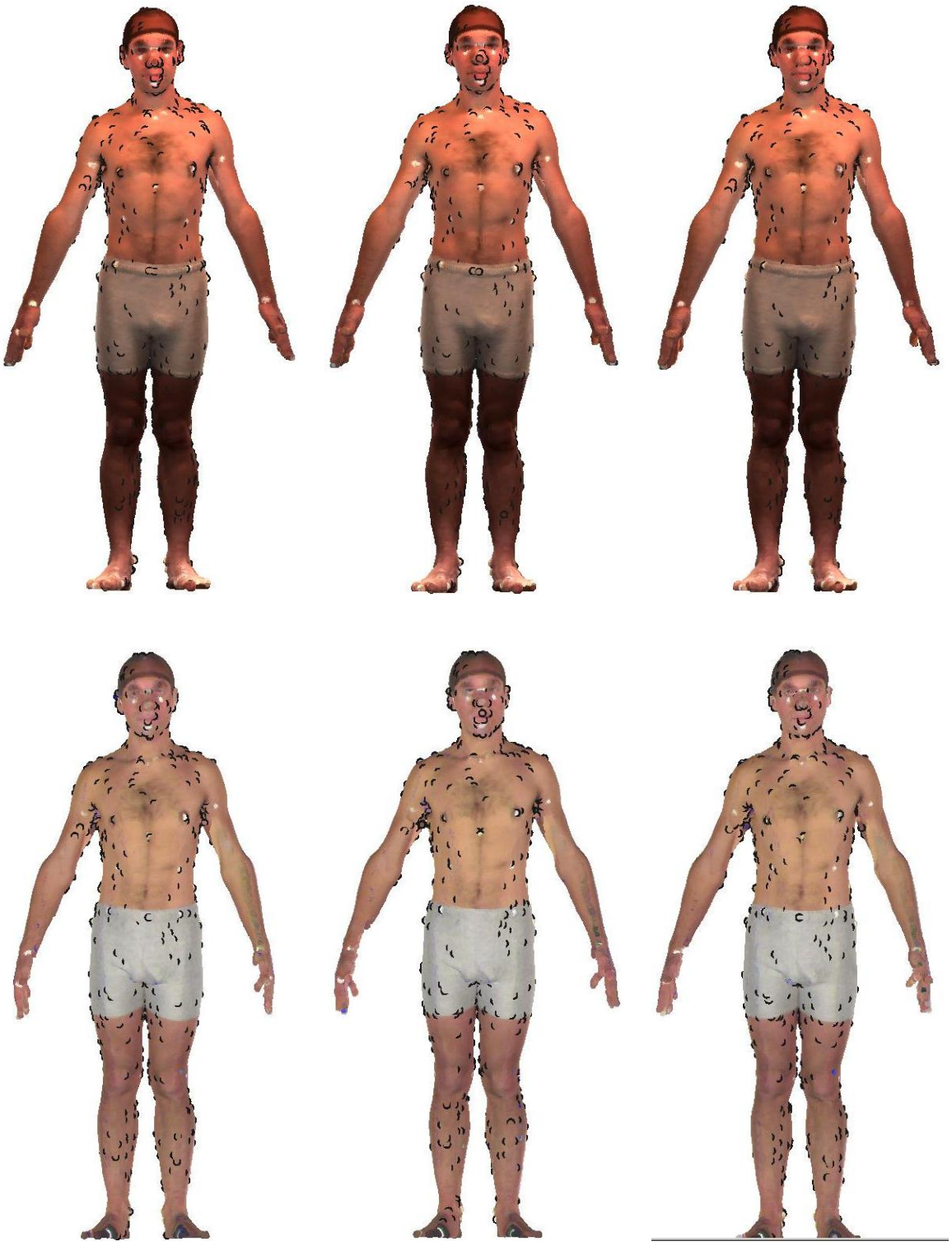

Figure 31 - Automatically selected intrinsic landmarks of a male subject, where the black dots mark selected landmarks, found in all six scans

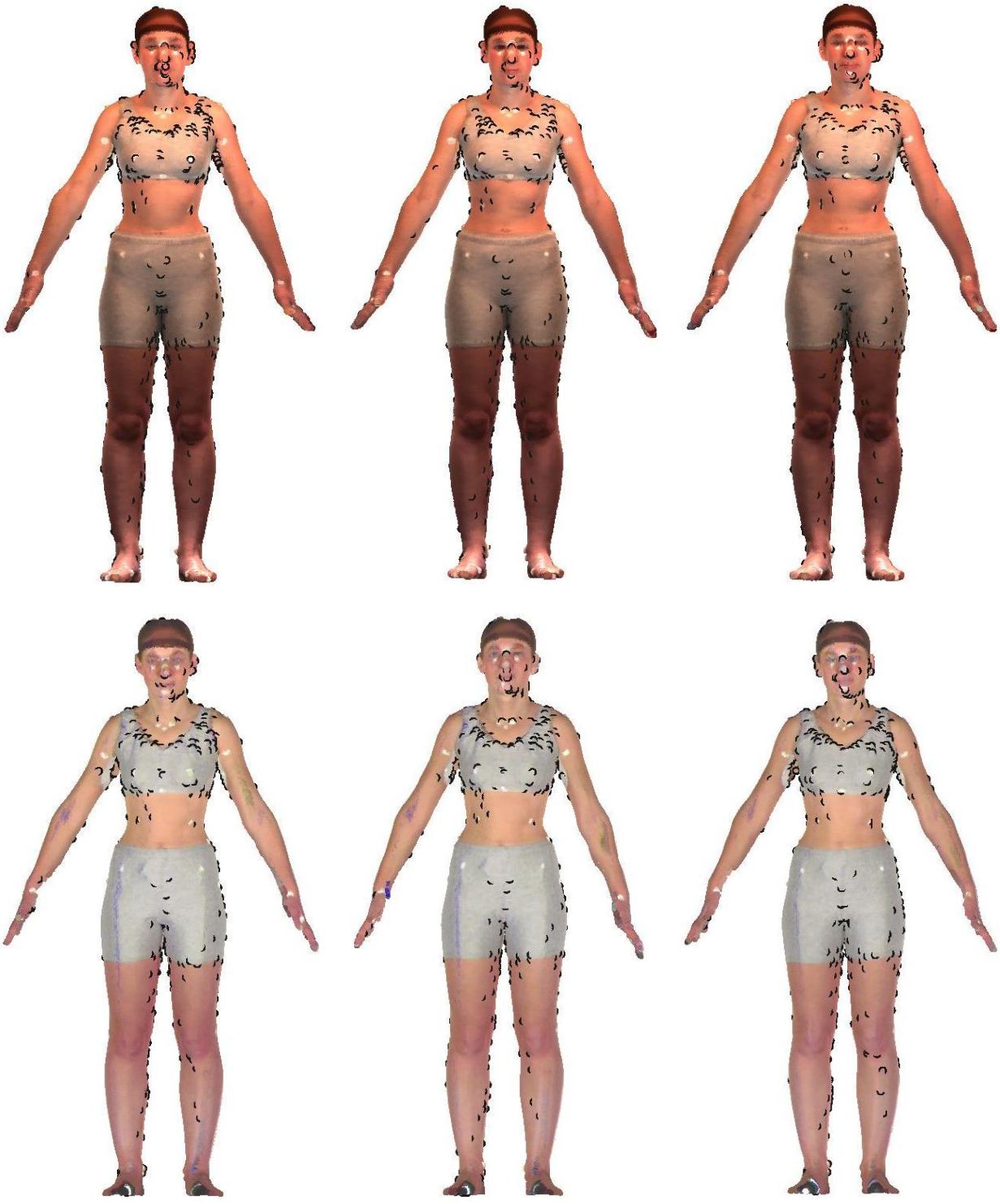

Figure 32 - Automatically selected intrinsic landmarks of a female subject, where the black dots mark selected landmarks, found in all six scans

4.2.6 Landmark Selection Results

Stable intrinsic landmarks were successfully selected for all twenty of the baseline scans. In Figure 31 and Figure 32, the selected landmarks for one male and one female model are presented. These are the retained feature points that were matched in all six scans. Considering all twenty models, on average 375 stable intrinsic landmarks were selected from an average of 2589 feature points.

Table 1 - Number of generated feature points and selected landmarks

Model	1	2	3	4	5	6	7	8	9	10
Initial Feature Points	2545	2976	2298	2921	2348	2533	2569	2211	2716	2147
Selected Landmarks	484	242	636	471	319	362	405	369	587	111

Model	11	12	13	14	15	16	17	18	19	20	Ave
Initial Feature Points	2433	2573	2761	2532	2430	2599	2875	2971	2330	3028	2589
Selected Landmarks	500	307	265	173	289	217	633	365	330	439	375

The selected landmarks were accurately matched, based on the results are given in Table 2 - Deviation values for selected landmarks. This table shows how closely the matched landmarks are clustered when transformed to the coordinate system of one model. The mean deviation for each model represents the average distances calculated for each selected landmark in that model. This distance is measured by calculating the centroid of the six matched landmarks, then

averaging the Euclidian distance between the centroid and each matched landmark. So, for Model 1, the mean deviation of each matched landmark from its cluster centroid is 7.80 *mm*, with a standard deviation of 0.01 *mm*. Overall, the mean deviation of matched landmarks from cluster centroid was less than 8 *mm*, with a standard deviation of 0.01 *mm*.

This selection of stable intrinsic landmarks achieves the first two objectives, which were as follows:

1. Given a set of range scans of a subject, select the same feature points in each scan of the subject.
2. Given a set of range scans of a subject, with feature points, select a number of stable landmarks specific to the subject.

This is the case, because, for each subject, at least 111 and at most 636 of the feature points were found in all scans of the subject. These feature points were selected as the stable intrinsic landmarks. Furthermore, the expectation that the number of retained feature points would trend to stable number of landmarks is supported by the graph in Figure 33. Each colored line represents a different subject. The left axis represents the percentage of feature points as each of the models (1 through 6 below) is analyzed. The most drastic drop-off is constantly at the point where the second model is considered, the drop-off for each subsequent model is significantly less. Based on these results, it is expected that of the original feature points generated, 15-20% of them will be retained as the stable landmarks. The graph is relatively flat at the sixth model; this indicates that the addition of more models will not result in a significant change in the selection of intrinsic landmark. Therefore, no more than six scans of a subject should be necessary and in many cases, only five may suffice for some applications.

Table 2 - Deviation values for selected landmarks

Model	Average Deviation from Mean (*mm*)	Standard Deviation of Deviation from Mean (*mm*)
1	7.80754	0.01463
2	7.48236	0.01436
3	7.70167	0.01408
4	7.56837	0.01372
5	7.55513	0.01355
6	7.66257	0.01408
7	7.70397	0.01492
8	7.50887	0.01435
9	7.74309	0.01415
10	8.04403	0.01444
11	7.52169	0.01371
12	7.63578	0.01406
13	7.56136	0.01421
14	7.38253	0.01361
15	7.83911	0.01478
16	7.69913	0.01357
17	7.54301	0.01353
18	7.64389	0.01446
19	7.44141	0.01394
20	7.59805	0.01402
Average	7.63218	0.01411

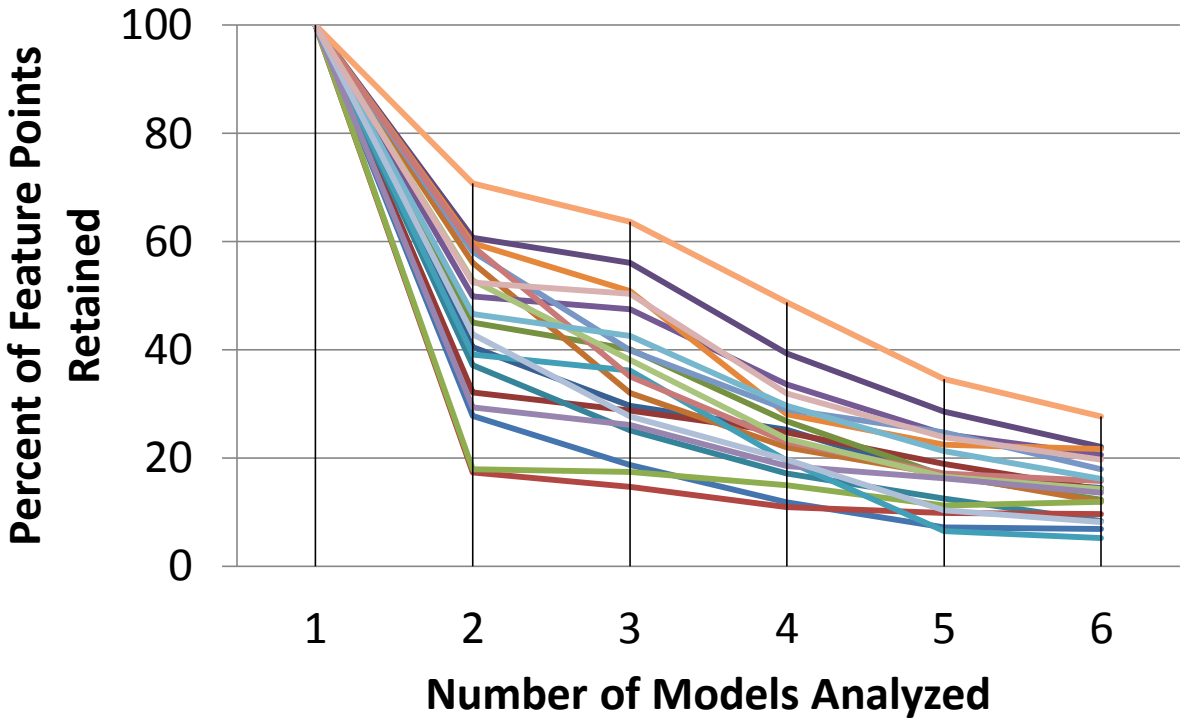

Figure 33 - Percentage of feature points retained after each model is analyzed

4.2.7 Landmark Selection Summary

Intrinsic landmarks were successfully selected for twenty baseline models. These stable intrinsic landmarks were selected from feature points located in every scan for the subject. The principal curvature value of each point and its surrounding region were calculated in order to generate those feature points for every scan. On average, several hundred landmarks were selected for each subject. Each landmark uniquely characterizes the local surface of the model and when combined with the location and number of landmarks, characterizes the model itself. In order to determine the utility of this characterization, these landmarks will be used to identify and characterize models.

4.3 Known Model Identification

In the previous sections, a method for selecting intrinsic landmarks and calculating descriptors in range scans was presented. These landmarks were selected in order to uniquely characterize each of the twenty baseline models. The utility of this characterization will be determined by using the landmarks to identify scans of the baseline models. This will address the third objective of the research:

3. Given a set of models, with a set of stable landmarks in each, identify new scans of those models.

The generation of the stable intrinsic landmarks analyzed each of the six scans for the twenty baseline models. In order to represent the identification of a new, unknown scan, the results of the previous section will have to be modified to exclude one of the six scans. The excluded scan will represent a new scan of a known model. In this paper, a "known" model will be considered to be a model with selected intrinsic landmarks. As demonstrated in the previous section, landmarks selected from a set of five scans contain a suitable number of stable intrinsic landmarks. So, landmark selection will be re-accomplished, this time using only five scans of each subject. The sixth scan will be excluded and considered a "new" scan. These new scans will be analyzed and identified, using intrinsic landmarks. Each analysis will be conducted independently and without any prior information, pre-specifications, or model marking used.

4.3.1 Landmark Selection

The landmark selection process for Known Model Identification mirrors the process used in the previous section. Each of five scans for all twenty baseline subjects was examined and the

feature points generated previously were used. However, the RANSAC process was only used to calculate transformations between the five scans. Feature points that were identified in all five scans were selected as stable intrinsic landmarks. Figure 34 displays the rate of retention for the feature points, as additional scans are considered. The percentage of retained feature points ranges from about 10% to almost 40%. This provides sufficiently stable landmarks for identification.

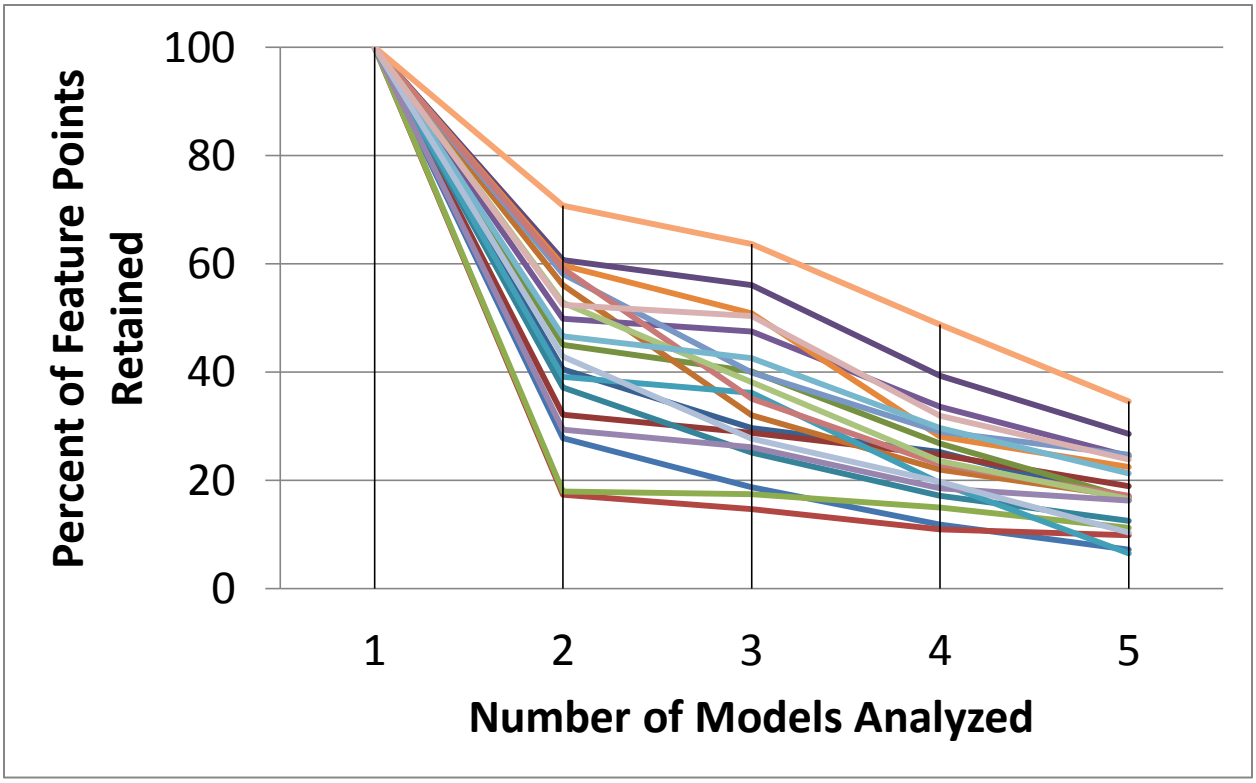

Figure 34 - Retained feature points using only five scans

4.3.2 Feature Point Generation

After the new stable intrinsic landmarks for the baseline models are selected, each of the new scans for the twenty baseline models were analyzed independently of one another. The new scans were examined as unidentified models and feature points were generated for each one.

The feature point generation process used was exactly the same as the one used previously. Feature points were selected based on the local strength of the maximum and minimum principal curvatures.

4.3.3 Transformation Calculation

Next, the new scan was compared to each of the twenty baseline models. These baseline models, one for each subject, contain the selected stable intrinsic landmarks and descriptors. Each landmark was located at the centroid of the matched feature points and was characterized by the descriptor containing the average principal curvatures of the matched feature points and the averaged curvatures for the surrounding regions. The transformation between the new model and each baseline model was calculated using the same RANSAC method presented earlier. In this step, however, four feature points from the new model were matched to stable intrinsic landmarks from the baseline model. If the transformation did not result in matches for at least 85% of the stable intrinsic landmarks, the process was repeated with four different feature points selected. Since the feature points of the new model were being compared to the stable intrinsic landmarks locations, the selection distance, ε, was reduced to 2.0 *cm*, resulting in closer matches and a reduced number of poor matches. The selection distance needed to be larger when comparing feature points, because every scan had a very large number of feature points and the only points that would be selected had to be matched across all scans of the model. In this case, the large number of feature points in the new model was being compared to the much smaller number of stable landmarks. Only feature points that aligned closely to the stable intrinsic landmarks were desired. When a suitable transformation was not able to be calculated, the transformation resulting in the highest percentage of matches was used. This was to be expected,

since two very different models were unlikely to share a large percentage of intrinsic landmarks. However, such transformations resulted in poor matches between feature points and landmarks, which were used to indicate that the new model was not a match to that baseline model.

4.3.4 Model Identification

Using the selected transformation, the feature points of the new model were transformed into the coordinate system of each baseline model. The percentage of matched intrinsic landmarks was recorded and compared for all twenty baseline models. The baseline model with the highest number of matched landmarks was selected as the identity of the new scan. A confidence score was calculated to represent how well the model matched and incorporated the quality of matches to the other baseline models. The initial score was based on the percentage of matched landmarks. It is highly unlikely that this percentage would ever approach 100%, since the matching criteria was set sufficiently tight. Even an attempt to identify one of the baseline scans used in the landmark selection would not result in a 100% match. That is because the baseline model contains the averaged landmark location and descriptors. The initial percentage is modified, depending on both the percentage of the next closest matching model and the average percentage of all the models that were not selected. The maximum possible confidence score was 100, representing the highest possible confidence in the identification. An identified model with a high percentage, such as 90%, of matched landmarks and with the next best match of only 60% matched landmarks, for example, would obtain a confidence score of 100. A confidence score of less than 85 indicates uncertainty in the identification.

4.3.5 Known Model Identification Results

This process was applied to all twenty new baseline scans, those that had been removed prior to landmark selection. Table 3 presents the results of the model identification. For nineteen of the twenty scans, the correct model was identified. In eighteen of the identifications, the confidence score was above 92 and over half scored the maximum. One model, number 13, was incorrectly identified as model 4, as seen in Figure 35 below. In this case the confidence score was very low, 76, and the selected model was the same gender with a similar body shape.

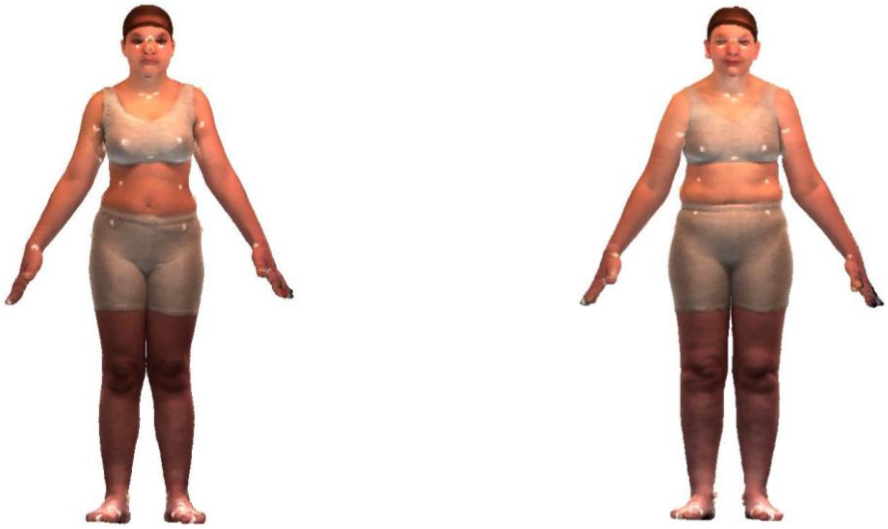

Model 13 Model 4

Figure 35 - Incorrect model identification

Table 3 - Know model matching results
(max confidence score = 100)

Model	Matched Model	Confidence
1	1	92
2	2	94
3	3	100
4	4	98
5	5	100
6	6	100
7	7	98
8	8	100
9	9	98
10	10	100
11	11	100
12	12	100
13	4	76
14	14	85
15	15	100
16	16	92
17	17	97
18	18	100
19	19	100
20	20	100
Average Confidence		96

4.3.6 Known Model Identification Summary

Given a set of 20 models, 10 male and 10 female, with 5 scans each, stable landmarks were selected, based on principal curvature characteristics. These stable landmarks were used to accurately and automatically identify new scans for nineteen of these models, with an average confidence score of 96 (out of 100). The entire process was automatic, requiring no user interaction or pre-specification. This is a novel and valuable functionality which achieves the third objective of this research:

3. Given a set of models, with a set of stable landmarks in each, identify new scans of those models.

4.4 Model Characterization

The identification of known models was presented in the previous section, demonstrating an application of intrinsic landmarks. The ability to identify known models is useful, but often, the scan subject is unknown, or not currently in the database. In these instances, it would be beneficial to use information about the known models to characterize the new, unknown subjects. This will address the fourth objective of the research:

4. Given a set of models, with a set of stable landmarks and known characteristics (i.e. gender, body mass index - BMI) in each, predict those characteristics in scans of new models with unknown characteristics.

The stable intrinsic landmarks selected from the set of all six scans for the twenty baseline models were used. One hundred scans were taken from the CAESAR database, 55 male and 45

female. These new, unknown scans will be analyzed and identified, using intrinsic landmarks. Each analysis will be conducted independently and without any prior information, pre-specifications, or model marking used. Characteristics will be predicted based on which of the known models the new scan most closely matches to.

4.4.1 Landmark Selection and Feature Point Generation

The twenty baseline models were used, each with the stable intrinsic landmark set developed, based on all six scans of each model. Each of the one hundred new CAESAR scans were examined as unidentified models and feature points were generated for each one. The process used was exactly the same as the one used previously. Feature points were selected based on the local strength of the maximum and minimum principal curvatures.

4.4.2 Transformation Calculation

Next, the new CAESAR scans were compared to each of the twenty baseline models. These baseline models, one for each subject, contain the selected stable intrinsic landmarks. Each landmark was located at the centroid of the matched feature points and was characterized by the descriptor containing the average principal curvatures of the matched feature points and the averaged curvatures for the surrounding regions. The transformation between the new model and each baseline model was calculated using the same RANSAC method presented earlier. In this step four feature points from the new model were matched to stable intrinsic landmarks from the baseline model. If the transformation did not result in matches for at least 85% of the stable intrinsic landmarks, the process was repeated with four different feature points selected. Since the feature points of the new model were being compared to the stable intrinsic landmarks locations, the selection distance, ε, was maintained at 2.0 *cm*, resulting in closer matches and a

reduced number of poor matches. Once again, when a suitable transformation was not able to be calculated, the transformation resulting in the highest percentage of matches was used.

4.4.3 Model Characterization

Using the selected transformation, the feature points of the new scan were transformed into the coordinate system of each baseline model. The percentage of matched intrinsic landmarks was recorded and compared for all twenty baseline models. The top five matches for each new model were used to predict the characteristics of the new scans. The gender characteristic was either 0 for male or 1 for female. BMI was calculated according to its definition, where BMI is mass (*kg*) divided by squared height (*m*). The characteristics of these five matches were averaged using weights based on the percentage of matched landmarks for each. This weighted average was used as the predicted BMI of the CAESAR scans and gender was selected as male if the gender average was less than 0.5, female if greater than 0.5, and undetermined at 0.5.

4.4.4 Model Characterization Results

The one hundred CAESAR models were processed and analyzed independently. The known characteristics for the CAESAR models and baseline models were obtained from metric data acquired at the time the subjects were scanned. The characteristics for the CAESAR models were only used to determine the accuracy of the predictions. For the fifty-five male models, the gender was accurately calculated in almost 90% of the models and BMI was accurately predicted to within about 94%. The predictions for the female models were less accurate, with gender predicated accurately only in 80% of the models and BMI predicted within about 87%. Overall, gender was accurately predicted almost 94% of the time, while BMI was predicted with a nearly 91% accuracy, as seen in Table 4.

Table 4 - Model characteristic results

Gender	Number	% of Genders Matched	BMI Accuracy
Male	**55**	**90.91%**	**93.85%**
Female	**45**	**80.00%**	**87.05%**
Average		**86.00%**	**90.79%**

The figures below each show a CAESAR model in the top left quadrant. The other quadrants contain three of the top matched baseline models as determined by the landmark match quality. Since the CAESAR subjects were not among the baseline model subjects, there cannot be an exact match. However, the match quality can only confirmed subjectively through a visual inspection. These are all positive matches for gender and the general body shape of the matches appear to agree as well. In general these top matches appear as slightly slimmer or larger than the CAESAR model under consideration.

4.4.5 Model Characterization Summary

Given a set of twenty models, each with stable landmarks and known features, a set of one hundred new and unknown models were successfully characterized. Gender was predicted with over 86% accuracy and BMI was predicted with over 90% accuracy. For these models, using intrinsic landmarks to predict unknown characteristics was successful, which achieves the fourth objective of this research:

4. Given a set of models, with stable landmarks and known characteristics (i.e. gender, BMI), predict those characteristics in scans of new models.

Figure 36 - CAESAR male 1 (top left), matching results

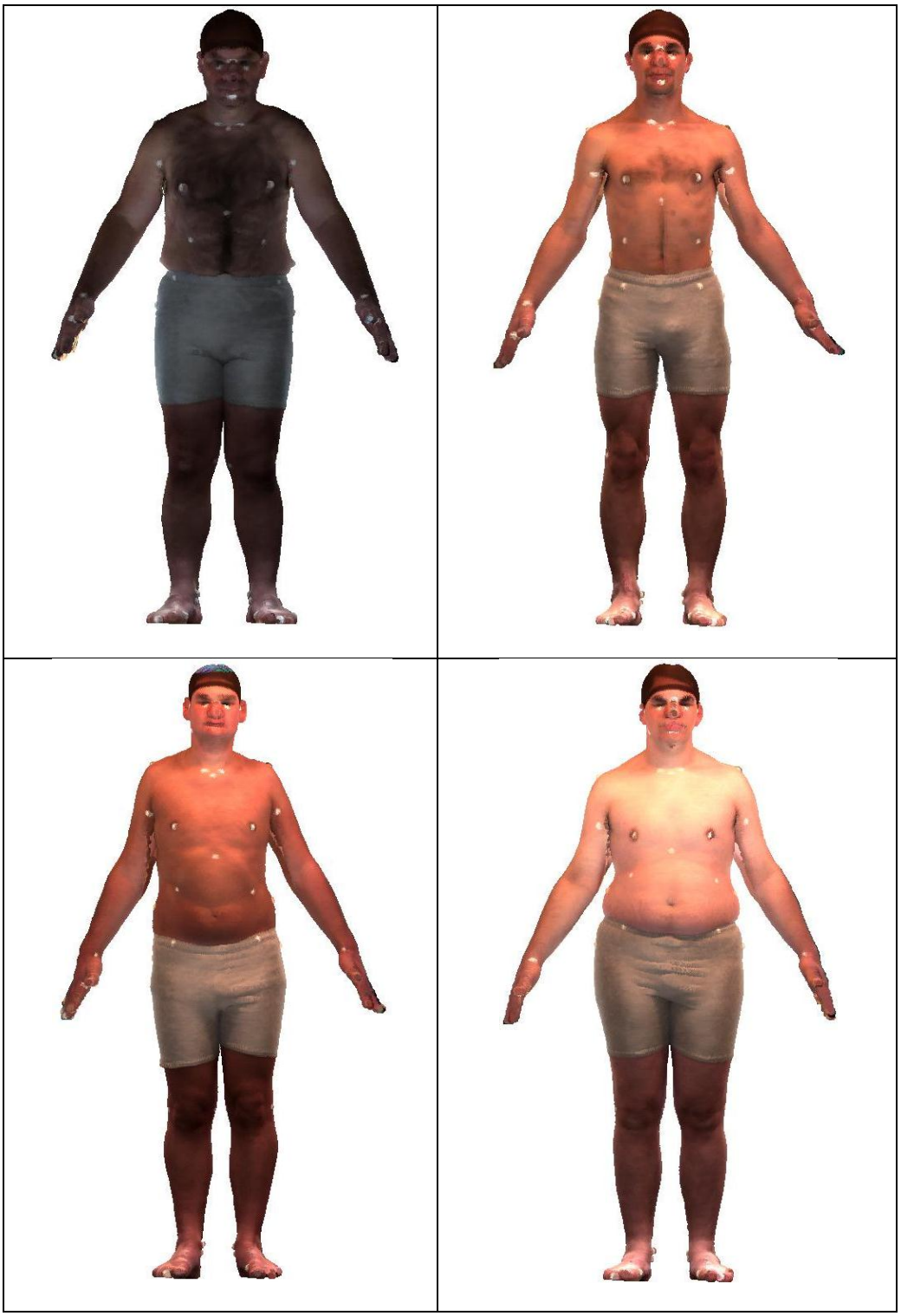

Figure 37 - CAESAR male 2 (top left), matching results

Figure 38 - CAESAR female 1 (top left), matching results

Figure 39 - CAESAR female 2 (top left), matching results

5 Contributions

Intrinsic landmarks are a novel approach in the characterization and identification of range scan models. This approach differs from previous efforts by using local characteristics of the model to determine the landmark locations, numbers, and descriptors. Using human models obtained from the Air Force Research Laboratory (AFRL), a baseline of twenty models were examined, intrinsic landmarks were selected and descriptors calculated. Additionally, the utility of these landmarks were demonstrated, as they were used to successfully identify known models and characterize unknown models.

It is important to note that the human body is not a rigid surface and that deformation and movement occurred between scans. However, the approach was still successful, and with a data set of rigid models, should be even more effective. The baseline data set contained only ten male and ten female models. This limited the range of models to use in matching the new, unknown CAESAR models used in the model characterization section of this research. Ideally, the database of known models, with selected intrinsic landmarks, would be much larger, with multiple models representing each naturally occurring body type. As range scanning technology develops further, the accuracy of the models will continue to increase, while the local noise should decrease. This would result in improved results, as the landmark descriptors would be more accurate.

Given a more robust database of known models and additional biometric and anthropometric expertise, intrinsic landmarks could be extremely useful in a variety of model identification and characterization applications. For example, given current airport security scanning implementations, subjects could be automatically checked to identify desired

individuals. Additionally, predictions on gender, weight, and possibly even ethnicity could be made and compared to visible characteristics, in order to identify discrepancies between the two. According to intrinsic landmarks, a matched model may have a much lower weight characteristic than recorded for the individual, indicating that there may be something heavy hidden in some way on or in the person.

Specifically this is a capability needed in studies conducted by the AFRL's Human Measurement and Signature Intelligence (MASINT) program. These studies have collected scans of several thousand subjects and will collect many more. Currently, they do not have the means to automatically characterize the models.

The use of intrinsic landmarks is not limited to human models. The process is applicable to any range scans stored as point clouds and triangular meshes. There a wide variety of potential applications for model characterization using intrinsic landmarks. Skeletal identification, especially for skulls, is one such application. The skulls of known subjects could be scanned to create a robust database of characteristics. The rigidity of the bones and rich research history makes this an ideal application for intrinsic landmarks. Additional applications could include such things as automotive identification or subject authentication.

6 Conclusion

A method for selecting intrinsic landmarks was introduced demonstrating encouraging results. Currently, the method can select these landmarks within mean deviation of about 8 *mm*. This is a useful capability that can be used to characterize and match any 3-D model set that is stored as a triangular mesh. The proposed method does not require any subject markings, specified landmark definitions, or user input; it is a fully autonomous system. The landmarks are characterized by a new, unique descriptor, containing the curvature properties of the local surface for each landmark.

The effectiveness of this new method and descriptor was presented. Each baseline model had an average of 375 intrinsic landmarks selected with descriptors. Known model were successfully identified using these landmarks for nineteen of the twenty baseline models, with a confidence score of 96 (out of 100) on average. New models, taken from the CAESAR database, had successfully predicted characteristics, based on matching intrinsic landmark properties. Gender was predicted correctly for 86% of the models, while BMI was predicted with nearly 91% accuracy. The successful identification and characterization results obtained in this research demonstrate the effectiveness of the intrinsic landmark descriptor and selection implementation.

This method provides a unique solution to a difficult problem in the study of range scans. Prior efforts have focused on landmark characterization based on traditional textile and manufacturing industry standard locations. Intrinsic landmarks are selected based on the local properties of the model and each has a defining descriptor, providing a unique characterization for each model. Landmarks are selected without any pre-specification or model knowledge and

the process does not require any user input or interaction at any point. Currently, there is not another method that can accomplish these results without pre-specifications or user input.

This research was initiated in support of the AFRL's Human Effectiveness Directorate, to provide a method for automatically characterizing range data using principal curvature values. The method has been successfully developed, providing encouraging results, identifying intrinsic landmarks in a data set of twenty baseline models. Based on these results this research is able to provide an innovative, rapid, and accurate method for automatically landmarks in 3-D range data.

7 Future Work

The initial effectiveness of intrinsic landmarks has been demonstrated. The method for selecting these landmarks was presented and the results were used to successfully identify known models and characterize unknown models. However, there is significant work that could be done to further develop the concept.

For the characterization of human models used in this research, the development of a larger database would be very beneficial. Obtaining at least five scans of subjects spanning the scope of BMI values and body shapes would provide the necessary details for predicting model characteristics. Additionally, subjecting the models to a strict anthropometric study could provide critical insight to the nature of the selected landmarks. Such a study could determine whether there are gender, size, ethnic, or other indicators apparent in the number and location of landmarks.

Additionally, the impact of significant deformation and movement on intrinsic landmarks should be studied. This would be to determine which landmarks remain consistent, which disappear, and which are modified in different positions. Furthermore, the ability to identify or characterize models in new poses could also be evaluated.

Finally, the application of intrinsic landmarks to new subject types could be investigated. As mentioned previously, the study of human skulls is a potential application. The research presented here could be applied to a database of skull models and similar evaluations implemented.

8 Appendix: Framework

The research code has been developed on Microsoft Windows operating system based computers. Coding was done both in MATLAB and Microsoft Visual Studio 2010 using a combination of C and C++. MATLAB was used primarily for independent data analysis as well as for data conversion and preprocessing. A PLY read and write package by Pascal Getreuer [**51**] was downloaded from the MATLAB support site. Additional MATLAB coding was written by the proposal author for this project. The bulk of the research code was written in Visual Studio, using standard OpenGL, the OpenGL Utility Toolkit (GLUT) [**52**] and several high-level math functions provided in The GNU Scientific Library (v1.14) for Visual Studio 2010 by Brian Gladman [**53**]. The project's code base was built using basic PLY file operations derived from code written by Greg Turk, GA Tech, provided by Dr. Arthur Goshtasby in several graduate courses and basic OpenGL graphics manipulation as developed in graduate courses with Dr. Thomas Wischgoll. The remaining code was written by the proposal author for this project.

8.1 Basic Functionality

The two preprocessing programs run autonomously, reading each data file in turn and saving the processed data in new folders. They are operated via minimal user-driven command prompt menus.

The primary landmark detection program provides a fully featured user interface, command prompt menus and a robust display built in OpenGL. Basic functions include opening, closing, importing and saving both PLY model files and data output files. PLY models can be viewed in 3-D with the original model colors. Rotation along the *x*, *y*, and *z* axis are possible as well as zooming in and out on the model. The model can be moved around the view screen by

mouse or numerical, directional keyboard input. An autonomous algorithm can be run to process batches of files, or models can be examined individually. Additionally, other autonomous algorithms can be run to learn the characteristics of selected landmarks from a set of models as well as to detect those landmarks in new models based off the learned characteristics. Curvature values for the entire model can be calculated and separately, feature points can be generated. It is possible to view the neighborhood of points around a selected point on the model along with the determined normal vector at that point. Alternatively, the neighborhood can be viewed in isolation, providing a demonstration of the fit of the calculated surface based on those neighbors, as well as the principal curvature directions, surface normal and the bin-clustering of neighborhood points. Once the curvature values have been calculated, the model can be seen as a color map of those values, ranging from blue areas of high negative curvature to orange areas of high positive curvature. Feature points can be displayed based on a number of input criteria and specific points can be selected to be included as landmarks. Finally, the size of the neighborhoods can be altered and new results calculated based on the new value.

9 References

[1] D. Eppstein, M. S. Paterson, and F. F. Yac, "On Nearest-Neighbor Graphs," *Discrete Computer Geometry*, vol. 17, pp. 263-282, 1997.

[2] Jagan Sankaranarayanan, Hanan Samet, and Amitabh Varshney, "A Fast All Nearest Neighbor Algorithm for Applications Involving Large Point-Clouds," *Computers & Graphics*, vol. 31, pp. 157-174, 2007.

[3] John Williams and Mohammed Bennamoun, "Simultaneous Registration of Multiple Corresponding Point Sets ," *Computer Vision and Image Understanding*, vol. 81, pp. 117-142, 2001.

[4] Shaoyi Du, Nanning Zheng, Shihui Ying, and Jianyi Liu, "Affine Iterative Closest Point Algorithm for Point Set Registration," *Pattern Recognition Letters*, vol. 31, pp. 791-799, 2010.

[5] Martin A. Fischler and Robert C. Bolles, "Random Sample Consensus: A Paradigm for Model Fitting with Applications to Image Analysis and Autmoated Cartography," *Communications of the ACM*, vol. 24, no. 6, pp. 381-395, June 1981.

[6] R. Hartley and A. Zisserman, *Multiple View Geometry in Computer Vision*.: Cambridge University Press, 2003, pp. 117-121.

[7] Martin Peternell and Helmut Pottmann, "A Laguerre Geometric Approach to Rational Offsets," *Computer Aided Geometric Design*, vol. 15, pp. 223-249, 1998.

[8] Sait Ismail Ozkaya, "QUADRO - A Program to Estimate Principal Curvatures of Folds," *Computers & Geosciences*, vol. 28, pp. 467-472, 2002.

[9] Carsten Lange and Konrad Polthier, "Anisotropic Smoothing of Point Sets," *Computer Aided Geometric Design*, vol. 22, pp. 680-692, 2005.

[10] W. F. Harris, "Curvature of Ellipsoids and Other Surfaces," *Ophthalmic and Physiological Optics*, vol. 26, no. 5, pp. 497-501, 2006.

[11] A. Ardeshir Goshtasby, "Grouping and Parameterizing Irregularly Spaced Points for Curve Fitting," *ACM Transactions on Grpahics*, vol. 19, no. 3, pp. 185-203, July 2000.

[12] A. Ardeshir Goshtasby, "A Weighted Mean Approach to Smooth Parametric Representation of Polygon Meshes," *The Visual Computer*, vol. 20, pp. 344-359, 2004.

[13] A. Ardeshir Goshtasby, "Plus Curves and Surfaces," *The Visual Computer*, vol. 21, pp. 4-16, 2005.

[14] Martin Peternell, "Developable Surface Fitting to Point Clouds," *Computer Aided Geometric Design*, vol. 21, pp. 785-803, 2004.

[15] Gregory M. Nielson, "Normalized Implicit Eigenvector Least Squares Operators for Noisy Scattered: Radial Basis Functions," *Computing*, vol. 86, pp. 199-212, 2009.

[16] Kim Kenobi, Ian L. Dryden, and Huiling Le, "Shape Curves and Geodesic Modelling," *Biometrika*, vol. 97, no. 3, pp. 567-584, 2010.

[17] Simon Flory and Michael Hofer, "Surface Fitting and Registration of Point Clouds Uing Approximations of the Unsigned Distance Function," *Computer Aided Geometric Desing*, vol. 27, pp. 60-77, 2010.

[18] Richard Szeliski and Stephane Lavallee, "Matching 3-D Anatomical Surfaces with Non-Rigid Deformations using Octree-Splines," *International Journal of Computer Vision*, vol. 18, no. 2, pp. 171-186, 1996.

[19] Yueqi Zhong and Bugao Xu, "Automatic Segmenting and Measurement on Scanned Human Body," *International Journal of Clothing Science and Technology*, vol. 18, no. 1, pp. 19-30, 2006.

[20] Osca Kin-Chung Au, Chiew-Lan Tai, Hung-Kuo Chu, Daniel Cohen-Or, and Tong-Yee Lee, "Skeleton Extraction by Mesh Contradiction," *ACM Transactions on Graphics*, vol. 27, no. 3, p. Article 44, August 2008.

[21] Tony Lindeberg, "Feature Detection with Automatic Scale Selection," *International Journal of Computer Vision*, vol. 30, no. 2, pp. 79-116, 1998.

[22] Karla Peavy Simmons, "Body Measurement Techniques: A Comparison of Three-Dimensional Body Scanning and Physical Anthropometric Methods," Raleigh, N.C., 2001.

[23] K. M. Robinette, H. Daanen, and E Paquet, "The CAESAR Project: A 3-D Surface Anthropometry Survey," in *Second International Conference on 3-D Digital Imaging and Modeling*, Ottawa, 1999.

[24] Dennis Burnsides, Mark Boehmer, and Kathleen Robinette, "3-D Landmark Detection and Identification in the CAESAR Project," 2001.

[25] Makiko Kouchi and Masaaki Mochimaru, "Errors in Landmarking and the Evaluation of the Accuracy of Traditional and 3D Anthropometry," *Applied Ergonomics*, vol. 42, pp. 518-527, 2011.

[26] Arzu Vuruskan, Bettina Seider, and Ute Detering-Koll, "Data Compatibility Analysis of 3D Body Scanning," in *2nd International Conference on 3D Body Scanning Technologies*, Lugano, 2011, pp. 338-348.

[27] (2011) Scan Worx Software. [Online]. http://www.scanworx.co.uk/index-2.html

[28] L. Dekker, I. Douros, B. F. Buxton, and P. Treleaven, "Building Symbolic Information for 3D Human Body Modeling from Range Data," in *Second International Confeernce on 3-D Digital Imaging and Modeling*, Ottawa, 1999, pp. 388-397.

[29] C. K. Au and M. M. F. Yuen, "Feature-Based Reverse Engineering of Mannequin for Garment Desigin," *Computer-Aided Desing*, vol. 31, no. 12, pp. 751-759, 1999.

[30] Brett Allen, Brian Curless, and Zoran Popovic, "The Space of Human Body Shapes: Reconstruction and Parameterization from Range Scans," *ACm Special Interest Group on Computer Graphics and Interactive Techniques*, vol. 22, no. 3, pp. 587-594, July 2003.

[31] Charlie C.L. Wang, "Parameterization and Parametric Design of Mannequins," *Computer-Aided Design 37*, 2005.

[32] Charlie C.L. Wang, Terry K.K. Chang, and Matthew M.F. Yuen, "From laser-scanned data to feautre Human Model: A System Based on Fuzzy Logic Concept," *Computer-Aided Design 35*, 2003.

[33] Iat-Fai Leong, Jing-Jing Fang, and Ming-June Tsai, "Automatic Body Feature Extraction from a Marker-Less Scanned Human Body," *Computer Aided Design 39*, 2007.

[34] Z. Ben Azouz, M. Rioux, C. Shu, and R. Lepage, "Analysis of Human Shape Variation Using Volumetric Techniques," *The 17th Annual Conference on Computer Animation and Social Agents*, July 2004.

[35] Z. Ben Azouz, M. Rioux, C. Shu, and R. Lepage, "Characterizing Human Shape Variation Using 3-D Anthropometric Data," *The Visual Computer International Journal of Computer Graphics*, vol. 22, no. 5, pp. 302-314, 2005.

[36] Z. Ben Azouz, C. Shu, and A. Mantel, "Automatic Locating of Anthropometric Landmarks on 3D Human Models," *Third International Symposium on 3D Data Processing, Visualization and Transmission*, June 2006.

[37] Z. Ben Azouz, C. Shu, R. Lepage, and M. Rioux, "Extracting main Modes of Human Shape Variation from 3-D Anthropometric Data," *Fifth International Conference on 3-D Digital Imaging and Modeling*, June 2005.

[38] A. E. Johnson and M. Hebert, "Recognizing Objects by Matching Oriented Points, Proc.," *Computer Vision and Pattern Recognition*, pp. 684-689, 1997.

[39] Mao-Jiun J. Wang, Wen-Yen Wu, Kao-Chao Lin, and Shi-Nine Yang, "Establishing Anthropometric Data from Whole-Body Scanner," in *Fifth Asia Pacific Industrial Engineering and Managment Systems Conference*, 2004, pp. 10.4.1-10.4.6.

[40] Jun-Ming Lu and Mao-Jiun J. Wang, "Automated Anthropometric Data Collection Using 3D Whole Body Scanners," *Expert Systems with Applications*, vol. 35, pp. 407-414, 2008.

[41] Hyunsook Han, Yunja Nam, and Su-Jeong Hwang Shin, "Algorithms of the Automatic Landmakr Identification for Various Torso Shapes," *International Journal of Clothing Science and Technology*, vol. 22, no. 5, pp. 343-357, 2010.

[42] David A. Hirshberg, Matthew Loper, Eric Rachlin, Aggeliki Tsoli, and Alexander Weiss, "Evaluating the Automated Alignment of 3D Human Body Scans," in *2nd International Conference on 3D Body Scanning Technologies*, Lugano, 2011, pp. 76-85.

[43] J. Paul Siebert and Stephen J. Marshall, "Human Body 3D Imaging by Speckle Texture Projection Photogrammetry," *Sensor Review*, vol. 20, no. 3, pp. 218-226, 2000.

[44] Gianluca Percoco, "Digital Close Range Photogrammetry for 3D Body Scanning for Custom-Made Garments," *The Photogrammetric Record*, vol. 26, no. 133, pp. 73-90, March 2011.

[45] Andrea Cardini, Anna-Ulla Jansson, and Sarah Elton, "A Geometric Morphometric Approach to the Study of Ecogeographical and Clinal Variation in Vervet Monkeys," *Journal of Biogeography*, vol. 34, pp. 1663-1678, 2007.

[46] Ashely L. Tamlin, Jeff Bowman, and David F. Hackett, "Seperating Wild from Domestic American Mink Neovison Vison Based on Skull Morphometrics," *Wildlife Biology*, vol. 15, pp. 266-277, 2009.

[47] Lijun Yin and Matt T. Yourst, "3D Face Recognition Based on High-Resolution 3D Face Modeling from Frontal and Profile Views," *Workshop on Biometric Methods and Applications*, November 2003.

[48] A. K. Ghosh and P. Sinha, "An Economised Craniofacial Identification System," *Forensic Science International*, vol. 117, pp. 109-119, 2001.

[49] Kathleen M. Robinette and Hein A.M. Daanen, "Precision of the CAESAR Scan-Extracted Measurements," *Applied Ergonomics*, vol. 37, no. 3, pp. 259-265, May 2006.

[50] Michael E. Mortenson, *Geometric Modeling*, Third Edition ed. New York, New York: Industrial Press Inc., 2006.

[51] Mathworks, Inc. MATLAB Central. [Online]. http://www.mathworks.com/matlabcentral/fileexchange/5459-read-write-ply-files

[52] Khronos Group. GLUT - The OpenGL Utility Toolkit. [Online]. http://www.opengl.org/resources/libraries/glut/

[53] Brian Gladman. The GNU Scientific Library. [Online]. http://gladman.plushost.co.uk/oldsite/computing/gnu_scientific_library.php